Bull. Spec. Astrophys. Obs., 58, 2005, 90-116

SCORPIO: prime focus reducer of the BTA

Afanasiev V.L., Gazhur E.B., Zhelenkov S.R., Moiseev A.V.

Special Astrophysical Observatory of the Russian AS, Nizhnij Arkhyz 369167, Russia

Received November 23, 2004; accepted December 12, 2004.

The focal reducer SCORPIO is described, which has been used for observations at the 6 m telescope of SAO RAS since the fall of 2000. We describe the features of the design and parameters of the device in different modes of observations (photometry, longslit and multi-slit spectroscopy, spectrophotometry and panoramic spectroscopy with a Fabry-Perot interferometer). Detailed characteristics of changeable equipment (filters, dispersers, etc.) are given. The capabilities of SCORPIO can be demonstrated by examples of observations of different astronomical objects.

Key words: instrumentation: miscellaneous

1. Introduction

The idea of using a system reducing the telescope focus length (a focal reducer) was proposed and implemented by Georg Courtés as early as the 50–60s of the last century (see, for example, Courtés 1960, 1964). The focal reducer executes several tasks simultaneously. Firstly, it increases the equivalent focal ratio and the field of view, which is important for investigation of extended objects. Secondly, the application of specially developed optics enables compensation off-axis abberations of the telescope's main mirror. Thirdly, a possibility appears to place dispersing elements (grisms, Fabry-Perot interferometer etc.) in a collimated beam between the collimator and the camera, which transforms the reducer to a multimode spectrograph.

Devices built with such a layout and intended, first of all, for spectroscopy and photometry of faint extended objects have been widely used for the last two decades. It suffices to name the EFOSC of the 3.6 m telescope of ESO (Buzzoni et al. 1984), which became, in many respects, a prototype of the present-day spectrographs of 8–10 m class telescopes, such as FORS at VLT (Nicklas et al. 1997).

The first focal reducer, which employed commercial photoobjectives, was made for interferometric observations with the 6 m telescope BTA at SAO RAS in the middle of the 80s. Despite the shortcomings (such as the poor image quality at the edges of the field of view, the low throughput of the optics (about 30% at a maximum) and the absence of automatization) the reducer had been s used on BTA until a question arose to improve it. In 1999 work was started over the creation of a new focal reducer for the prime focus of BTA. The new device SCORPIO (**S**pectral **C**amera with **O**ptical **R**educer for **P**hotometric and **I**nterferometric **O**bservations) enables the following modes of observations of extended and starlike objects at the BTA prime focus:

- CCD photometry in broad-, medium- and narrow-band filters.
- Panoramic spectroscopy with the Fabry-Perot interferometer.
- Long-slit spectroscopy.
- Slitless spectroscopy.
- Multiobject spectroscopy with 16 slits moved remotely in the focal plane.
- Polarimetry in the filtres and spectropolarimetry.

The first observations at the BTA were conducted with the old version of the prime focus adapter in 2000 September. The new platform-adapter was placed in service in May, 2001. The first successful spectral observations with the multi-slit unit were carried out in September, 2003. In the summer of 2004 work was completed on introduction of a spectropolarimetric mode and the first observations were made.

Mechanical and optics of the SCOPRIO were manufactured at the workshop of SAO RAS by the project of V.L. Afanasiev and E.B. Gazhur. The optics of the spectrograph was made by E.I. Perepelitsyn following the calculations V.L. Afanasiev. The assembly of the mechanical parts of the device was performed by V.V. Veretenov. The remote control boards

Table 1: *The main characteristics of SCORPIO*

Total focal ratio	$F/2.6$
Field of view:	
full [1]	$6.1' \times 6.1'$
in mutlsilit mode [1]	$2.9' \times 5.9'$
Image scale [1]	$0.18''$/pixel
Spectral range	$3\,600 - 10\,000$Å
Spectral resolution	
with grisms	
(for slit width $1''$)	$1.5 - 20$Å
with Fabry-Perot	
inteferometers	$0.8 - 2.5$Å
Maximal quantum efficiency	
(telescope+SCORPIO+CCD)	
Direct imaging	70%
Spectroscopy	40%
Observations with IFP	20%

[1] for the detector CCD EEV-42-40

of the device were designed and made by S.R. Zhelenkov, while the electronical part was a creation of V.I. Fateev. The control software was written by A.V. Moiseev.

The features of the design of the device and the procedure of observations with it at the BTA are sequentially described below. The optical-mechanical design of the SCORPIO, incorporating the focal reducer, prime focus platform-adapter and CCD detector are considered in Section 2. The characteristics of changeable optical equipment (filters, prisms etc.) are presented in Section 3. The system of remote control of the spectrograph are described in Section 4. The features of observations in different modes are considered in Section 5, there are also given examples of some observational results obtained at the 6 m telescope during the test operations of the device. Section 6 gives some recommendations concerning the data reduction. The prospects of further updating of the SCORPIO are briefly discussed in Section 7.

2. Description of the spectrograph

Fundamental characteristic features are collected in Table 1. The SCORPIO consists of three main units, each of which can be used independently: the focal reducer, the prime focus platform-adapter and the CCD detector. The focal reducer includes the optics of the spectrograph and the multi-slit unit. The platform-adapter contains the optics and lamps for the calibration of the spectrograph, two fields to search for guiding stars, a TV-viewing system and a tilted plate of fused quarts for fast guiding (tip-tilt)[1].

2.1. The focal reducer

The optical design of the focal reducer (Fig. 1) incorporates the lens of the field and the collimator — four-lens apochromat ($F/2.2$) with a focal length of 160 mm, forming the exit pupil of the system, camera objective — six-lens apochromat ($F/1.8$) with a focal length of 109 mm and changeable optical equipments — IFP, diffraction gratings, filters, polarization analyzer, phase plates, masks and slits. The equivalent focal ratio of the system at the prime focus of the 6 m telescope is $F/2.6$. All optical surfaces are coated with seven antireflecting layers in the range $3\,600 - 10\,000$ Å. The antireflecting layers are applied in Nizhnii Novgorod Institute of Applied Physics. Results of laboratory measurements of the SCORPIO optics spectral curve are given in Fig. 2.

The optics of the reducer is designed with the aid of the package ZEMAX and optimized for the real images obtained at BTA, which are on average $1.5''$. This allowed a sufficiently large field of view of the instrument to be realized without using of aspheric surfaces in the optical design. For the apochromatization in the visible wavelength range, a combination of glasses STK-12 and OK-4 was used, which have a difference of Abbe numbers of more then 37. A spot diagram of the SCORPIO computed for the entire optical path with allowance made for aberration of the main mirror of the BTA is displayed in Fig. 3. The optics of the collimator compensates for the coma and curvature of the field of the main mirror of the telescope, which makes it possible to reject the use of the standard BTA lens corrector without an antireflection coating in observations. The energy distribution at different distances from the center of the field of view is shown in Fig. 4. As can be seen from Fig. 3, the optics of the SCORPIO has residual astigmatism at the edge of the field of view, which actually has no effect on the image quality at seeings of 1.5-$2''$. At seeing better than 1-$1.5''$ the working field of view diminishes to 4 arcmin. Aberrations of the objective of the camera are corrected for a flat field of 30×30 mm, and the actual PSF does not exceed 50μm in the working spectral region. Fig. 5 shows dotted diagrams of the instrument when operating under spectral mode with a grating of 300 gr/mm. As it follows from the calculation the secondary spectrum of the SCORPIO does not exceed 100μm, while the chromatism of the position is no larger than $0.5''$ at the edge of the field throughout the visible wavelength range.

[1] Work on manufacturing system of fast guiding is planned to finish in 2005.

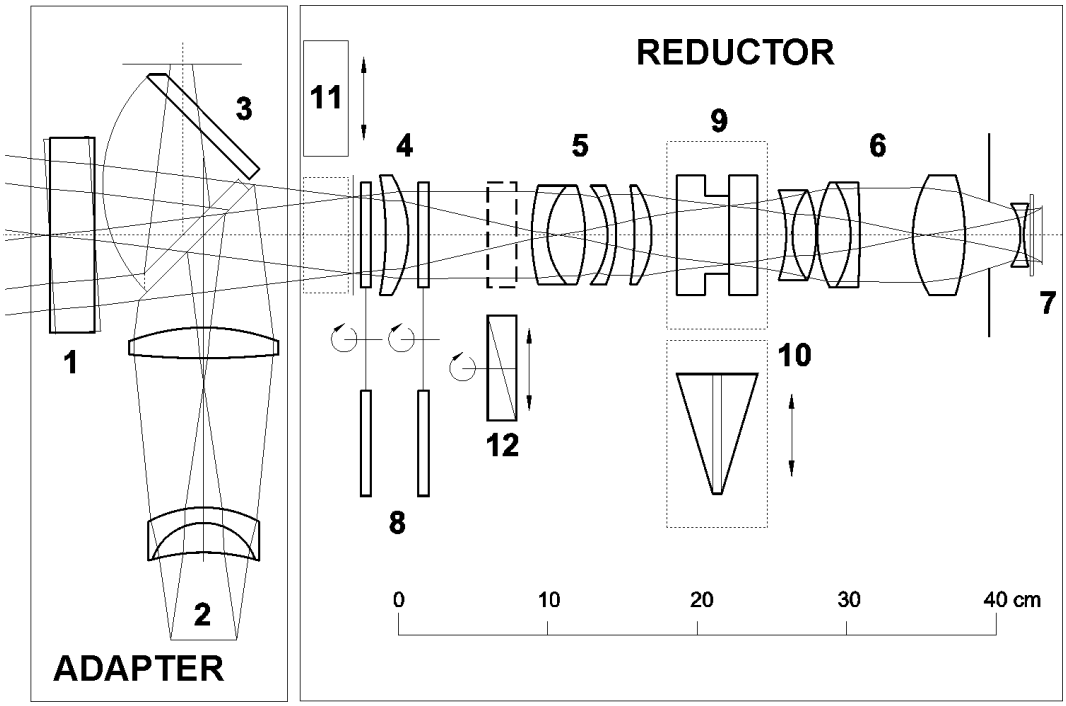

Figure 1: *Optical design of the SCORPIO. (1) – tip-tilt plate, (2) – calibration optics, (3) – flat mirror, (4) – field lens, (5) – collimator, (6) – camera, (7) – CCD, (8) – filter wheels, (9) – IFP, (10) – grism, (11) – multi-slit unit, (12) – polarization analyzer.*

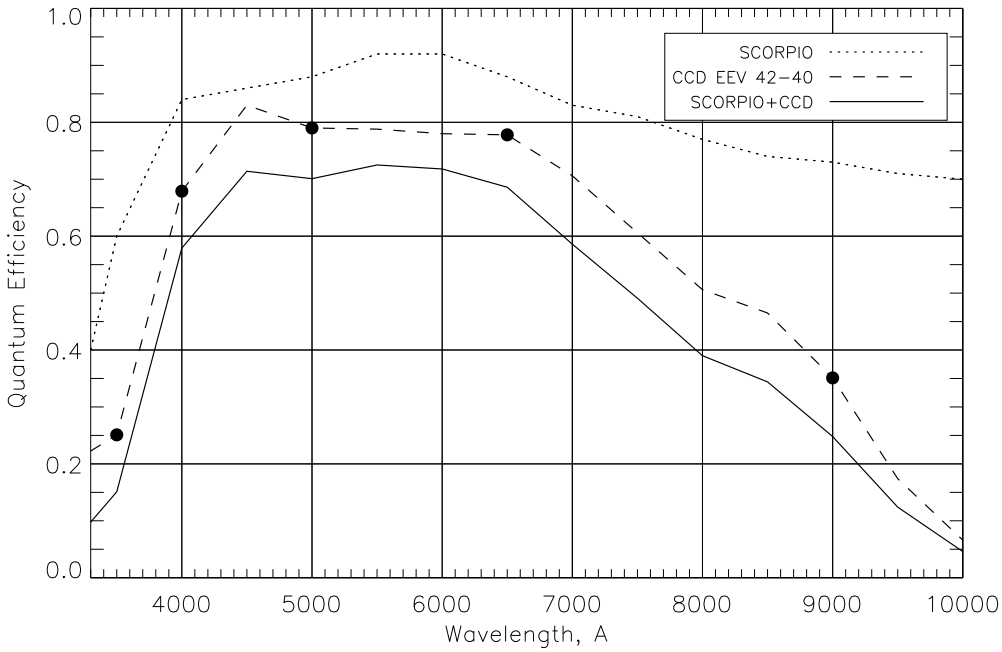

Figure 2: *Transmission curve for the the SCORPIO optics, the quantum efficiency curve for the CCD EEV-42-40 and the total quantum efficiency (SCORPIO+CCD). The filled circles mark the values provided by the manufacturer, the dotted line corresponds to the normalized curve for an analogous CCD used at the telescope TNG.*

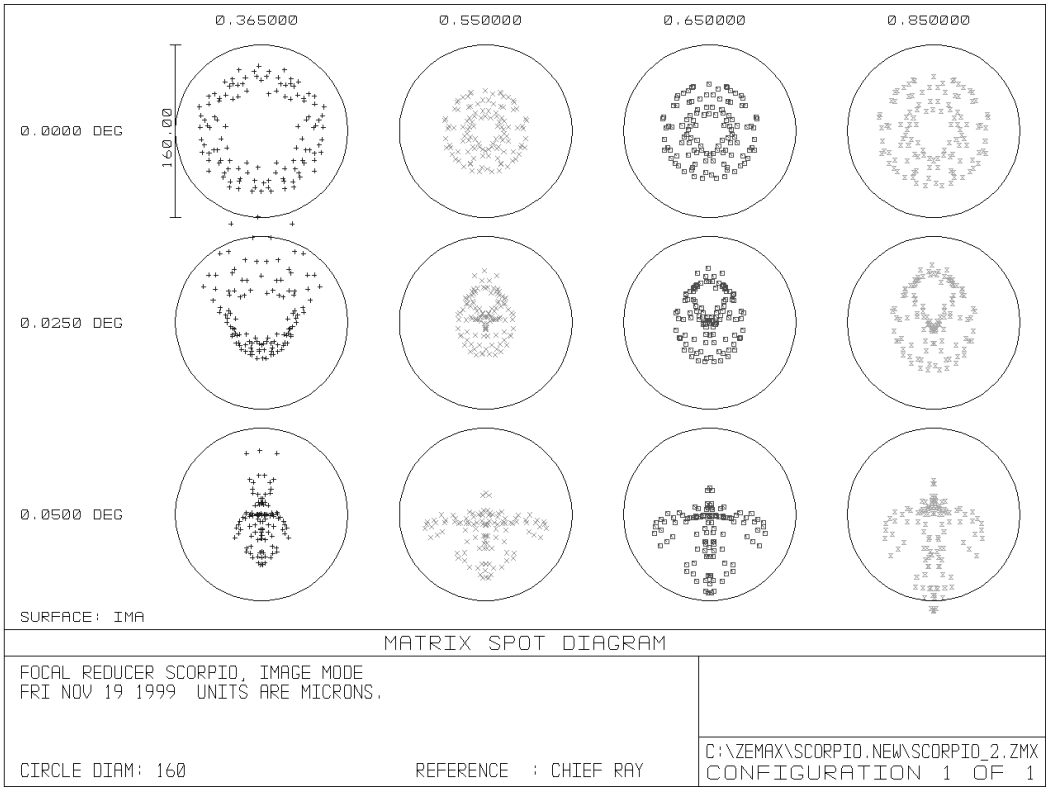

Figure 3: *Spot diagrams of the SCOPRIO optics at the focal plane of a CCD in the direct imaging mode in B, V, R, I bands. The circle's diameter is 2″.*

A displacement of the exit pupil from the last surface of the collimator is equal to a distance of 60 mm. The distance between the last lens of the collimator and the first one of the camera objective is 90 mm. The collimated beam diameter is 40 mm. The working distance of the camera is 14 mm. The equivalent focal length of the reducer installed on BTA makes 15.6 m, which corresponds to a scale of the image of $75\mu m/''$. The linear size of the non-vignetting field of view is 28×28 mm in the plane of the detector.

Constructively, the reducer is made in the form of separate units mounted in a common housing and located in the following order (reckoning from the front flange):

- multi-slit unit placed in front of the focal plane;
- two rotating wheels containing filters and slits;
- polarization analyzer placed in front of the collimator;
- collimator focusing mechanism;
- the mechanism of placing/removal of the dispersive element in/from the collimated beam.

The reducer incorporates two wheels with six positions ("0"..."5") to place in the beam different changeable units — filters, slits, masks etc. Wheel 1 is installed in the focal plane of the telescope, while Wheel 2 — is placed behind the field lens in front of the collimator. Wheel 1 usually holds medium- and narrow-band interference filters and also a slit for spectral observations (position "3"). Wheel 2 contains broad-band glass filters and masks for slitless spectroscopy (position "5"). All the elements mounted in the wheel are in bayonet holders allowing them to be readily changed. Position "0" in each of the wheel always remains vacant, so that all the mounted filters could be used in observations.

Between the collimator and camera there is a unit with two switchable positions (numbers "0" and "1") for placing the dispersion elements (Fabry-Perot interferometers or a grism) into the parallel beam. In so doing, the grisms may be fastened in position "0" only, while, the IFP — in position "1" alone. A neon lamp, mounted on a movable bracket, and a rigidly fixed diagonal mirror are provided for the visual check of the accuracy of tuning of the IFP removed from the beam.

The focusing of the camera objective is performed manually with the aid of a micrometric screw. The setting of the collimator is equipped with a step mo-

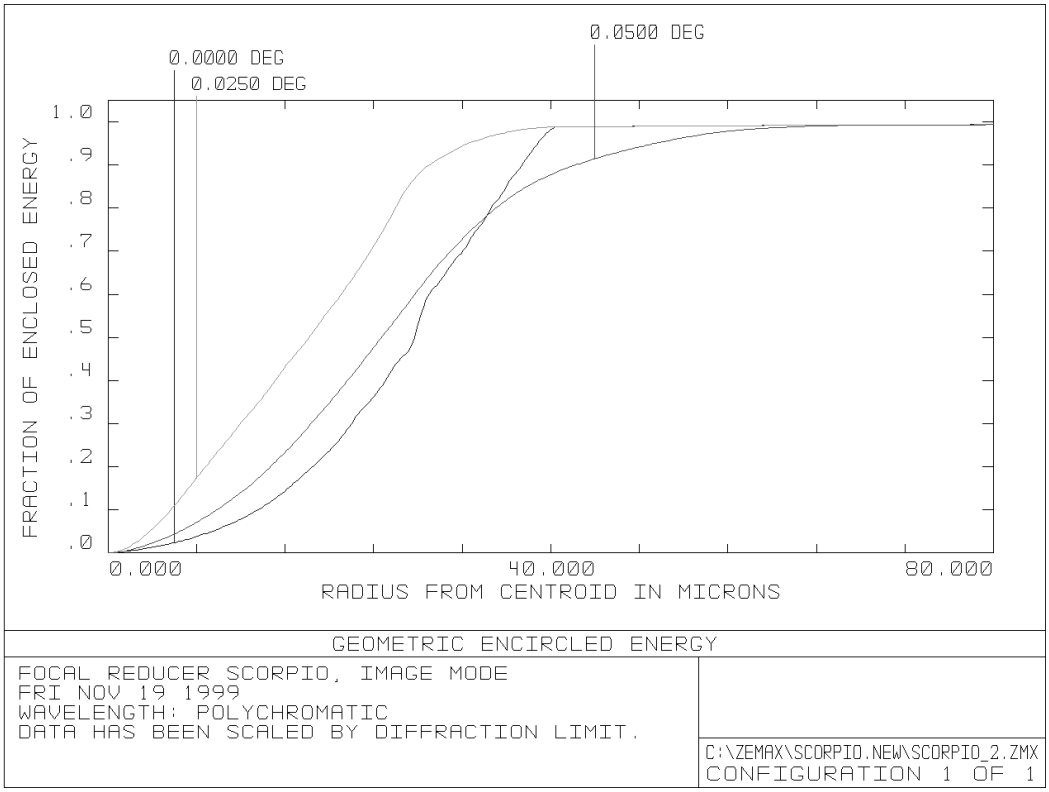

Figure 4: *Polychromatic energy distribution in a PSF of the SCORPIO in the focal plane of a CCD for a source size of 1″. The scale is 75 μm/″.*

tor to allow remote focusing. The focusing mechanism of the collimator ensures its linear movement within 12 mm with a precision of 0.01 mm. On the front (nearest to the main mirror) flange of the device there is the central electromagnetic shutter with a time of operation of 0.1 s.

2.2. Multi-slit unit

The multi-slit unit is installed inside the focal reducer near the focal plane of the telescope for permanent use (Fig. 1). It consists of 16 metal strips with slits movable in a field of $2.9' \times 5.9'$ (Fig. 6). The height of the slits is about $18''$, the distance between the centers of the slits is about $22''$. The position of each slit is fixed with two electromagnets — holding and catching. The holding magnets are fixed immovable, the catching ones are fastened on a frame moving in one coordinate with the aid of the step motor. The resistance of the electro magnets is about 90 Ohm, the voltage in the holding magnets is 5 V, in the catching ones it is 12 V. An individual magnet fixes the position of all the slits in the focal plane simultaneously. The device is put in the beam by means of the step motor. The time of complete arrangements of all the slits (a required accuracy $0.2 - 0.3''$) is about 10 minutes.

Table 2: *The λ/4-plate parameters*

λ, Å	phase shift, °	angle, °
3800	81.4	-4.1
4000	87.1	-1.3
4500	90.0	-0.3
5000	90.7	0
5500	91.0	-0.3
6000	91.3	-0.5
6500	91.5	-0.5
7000	91.4	-0.5
7500	90.6	-0.3
8000	88.7	-0.1

2.3. Spectropolarimeter

As the analyzer of linear polarization a Savara plate 14 mm thick is used, which ensures the divergence of the beam in two mutually perpendicular polarization planes by 9 arcsec in the focal plane. The analyzer can rotate around its axis assuming two fixed positions with angles of rotation of 0 and 45°. The placing-

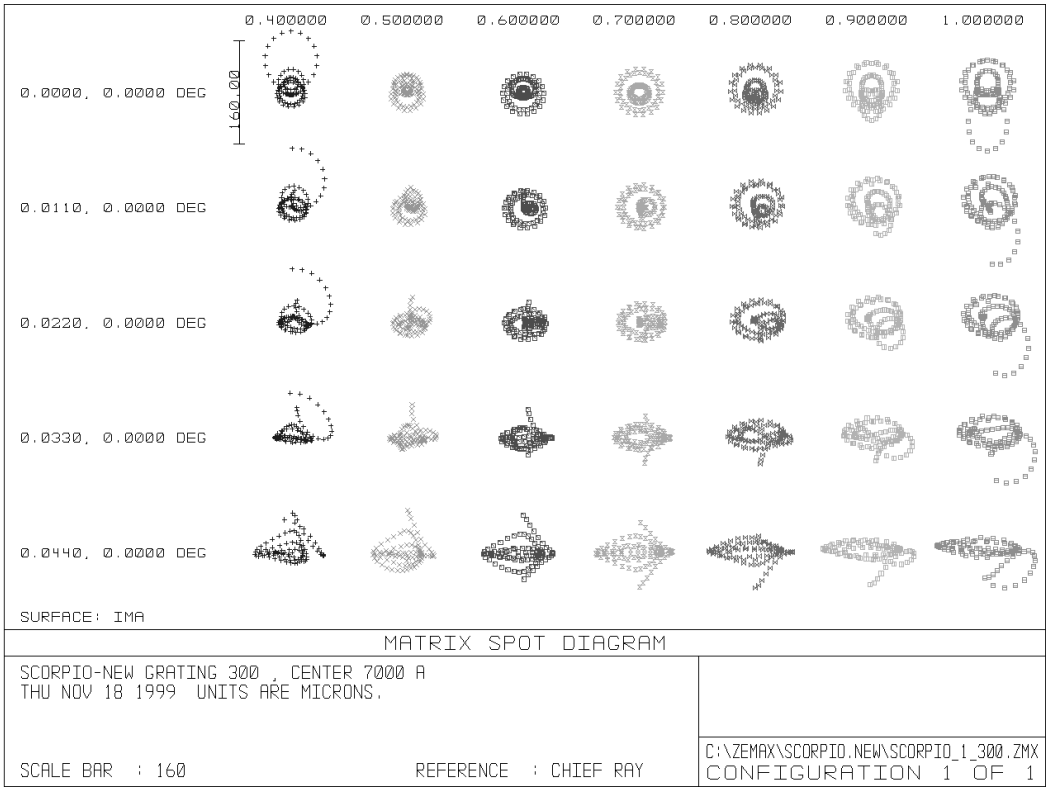

Figure 5: *Spot diagrams of the SCOPRIO optics at the focal plane of a CCD in the spectral mode for source size of 1″ and a grating of 300 gr./mm.*

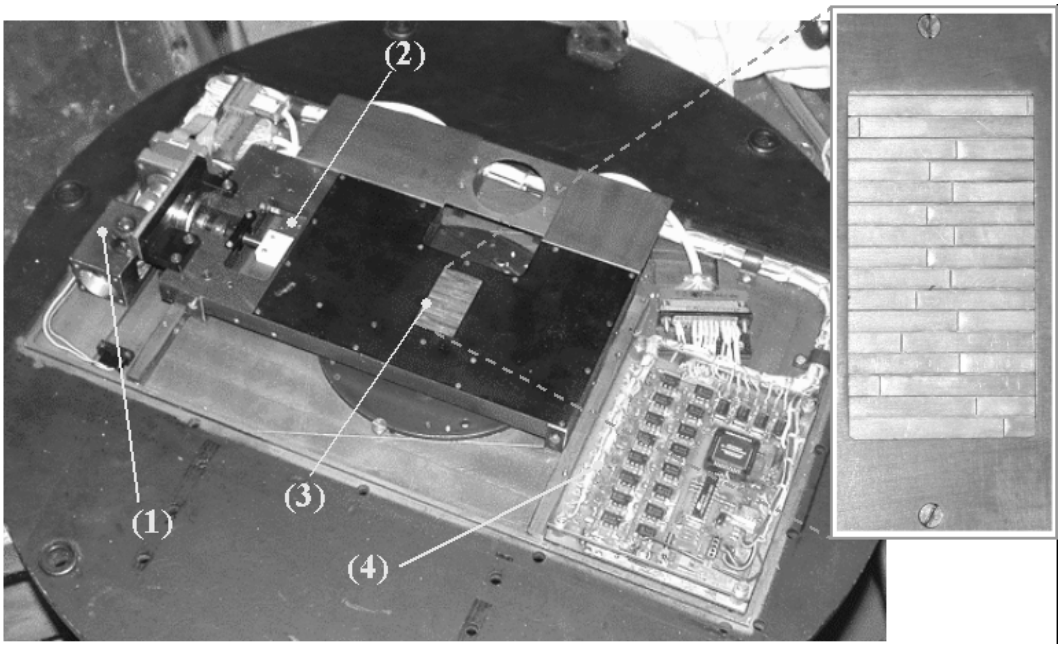

Figure 6: *A photography of the multi-slit unit. (1) – mechanism of putting the unit in the beam; (2) – movable frame with the catching magnets; (3) – steel strips with the slits (see the right zoomed photo); (4) – control board with a microprocessor.*

removing of the analyzer in and out of the light beam and its rotation are executed by a step motor. For measuring circular polarization a quarter-wave plate 6 mm thick is placed in the second wheel, which is achromatized in the range 3800–8000 Å. Table 2 contains the main characteristics of this plate: the phase shift and the angle of deviation of the optical axis at different wavelengths.

2.4. Prime focus adapter

The platform-adapter is attached to the turning table in the BTA prime focus and used for guiding by off-axis stars and for illuminating the spectrograph by calibration lamps. Both the focal reducer and other devices, for instance, the spectrograph MPFS, can be installed on it.

The adapter contains two rectangular fields to search for guiding stars[2]. The centers of the fields are offset by $12'$ from the center of the field of view. A fiber bundle displaced by step motors in a rectangular coordinate system is located in each of the fields (see Fig. 7). The off-axis lens corrector placed in front of each guiding field corrects the coma of the telescope's primary mirror. The equivalent focal length when using the corrector is 19.2 m, so a distance of $10.7''$ in the sky corresponds to moving of the bundle by 1 mm. The range of displacement of fiber bundles is $8.5' \times 4.5'$, the diameter of the field of view of each bundle is about $40''$.

The flat diagonal mirror (denoted as (3) in Fig. 1 and (2) in Fig. 7) has two fixed positions: "Fibers" and "Field". In the position "Fibers" the mirror throws the images from the fiber bundles to the TV viewing system. This mode is used when exposing objects. In the position "Field" the mirror blocks the central beam of light from the telescope and sends the image of the center of the device field of view to the TV viewing system. This is needed to roughly point the telescope at the required object. The field size on the TV guide is $3' \times 2'$. In addition, the light from the calibration lamps is directed to the spectrograph at this position of the mirror. The images of the crosses with tunable highlight are projected onto the center of the field of view and the centers of the bundles.

The optical design of the adapter contains the optics of the illuminator of calibration (Fig. 1), which forms a converging beam with the focal ratio equivalent to that of the telescope, $(F/4)$, at the entrance of the reducer. Such a scheme of the path of calibration forms the pupil of the system in the same position where the image of the telescope mirror is located, which allows not only correct calibration of the wavelength scale by the lamp of line spectrum, but also the calibration of the system throughput over the field under different modes of operation ("flat field") to be performed.

The entrance field of the calibration beam is illuminated via the integrating sphere (Ulbricht sphere) by two calibration lamps: with He-Ne-Ar filling for the wavelength calibration (hereafter the lamp NEON) and a halogen continuous spectrum lamp to produce a flat field (hereafter the lamp FLAT).

To speed up the process of pointing and search for guiding stars, we used a custom-developed software IDENTSTAR written in the IDL environment, which calculates the current instrumental coordinates of the guiding stars from the data sent by the BTA control computer.

Positions and stellar magnitudes of stars in this field are determined from the catalog USNO2.0. Fig. 8 shows the interface of the program of search for stars. The program selects the brightest stars in the limits of movement of the fields of guiding. When necessary, an observer has a possibility of choosing other stars in the interactive mode. Instrumental coordinates of stars are transmitted to the program controlling the reducer and platform. As a rule, the time of search of guiding stars does not exceed 3–5 minutes.

2.5. CCD detector

From 2000 to 2003 a CCD array TK1024 of 1024×1024 pixels was used as the detector. Since 2003 April, a CCD chip EEV-42-40 of 2048×2048 pixels has been used. The main parameters of the two detectors are collected in Table 3.

It should be noted that program selection of modes characterized by different values of gain, readout rate and noise is possible for EEV-42-40. Fig.2 displays a curve of quantum efficiency for EEV-42-40. The diagram is drawn on the basis of the data presented by the makers of the chip (filled circles in the figure) and the normalized curve of quantum efficiency for an analogous CCD operating at the telescope TNG.

The detectors are cooled by liquid nitrogen. The time the supply of nitrogen in a cryostat is consumed makes 12–13 hours for TK1024 and 20–22 hours for EEV-42-40. All the equipment needed for observations with a CCD (cryostat, electronics and remote control software) was developed and made in the Laboratory of Advanced Design of SAO RAS (*http://www.sao.ru/hq/adlab/*).

As one can see from Table 3 the detectors have a

[2] Since the 6 m telescope has an altazimuth mounting, both the position of the telescope in A and z and the rotation of the field of view should be controlled during the guiding. Therefore, two guiding stars are used.

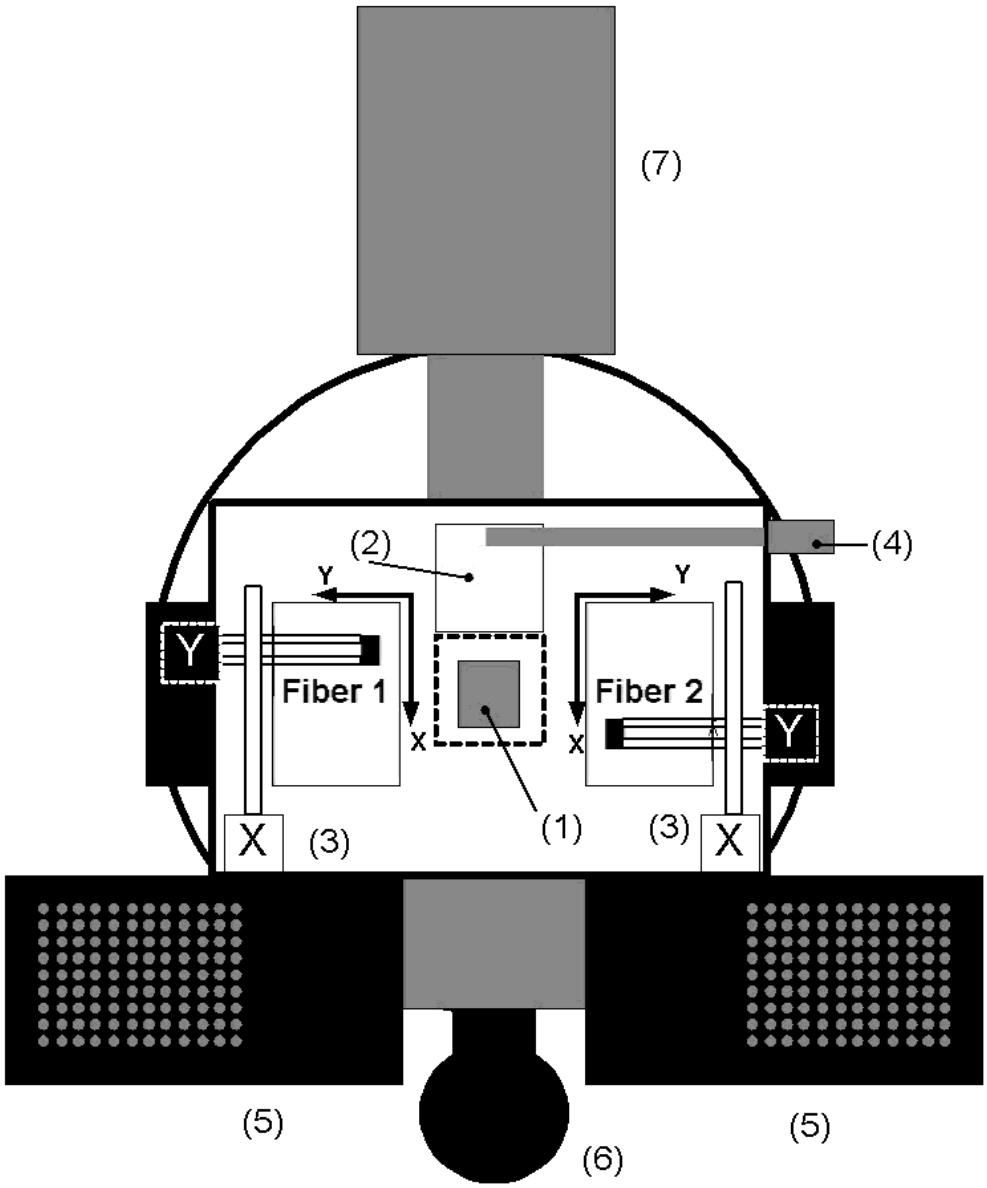

Figure 7: *The prime focus platform-adapter (view from the BTA main mirror direction). (1) – shutter, (2) – flat mirror, (3) – mechanisms for guiding bundle motions, (4) – crosses' lighting, (5) – power units and control board, (6) – integration sphere with lamps NEON and FLAT, (7) – TV viewing system.*

high quantum efficiency, low noises and low dark current. Besides, both detectors have nearly ideal "cosmetics": a small number of "bad columns" and "hot pixels". Very likely, the only shortcoming is the interference of the incidence light ("fringes"), which is observed at wavelength longer than 7500 Å for the CCD TK1024 and longer than 6600 Å in the case of EEV-42-40. An appropriate procedure of observations is needed for correct extraction of the interference pattern (see Sect. 6).

3. Changeable equipment

3.1. Slits and masks

The long slit for spectral observations is mounted in position "3" of Wheel 1. The slit width is fixed - 1″, the length is about 6′, i.e. it covers the whole field of view. At the desire of a user, a slit of arbitrarily changed width or a mask forming a dash slit for spectropolarimetric observations can be mounted. In the latter case, the height of each small slit is 7.5″, and the distances between the centers of the slits is 9.8″. The dashed slit is usually set in position "5".

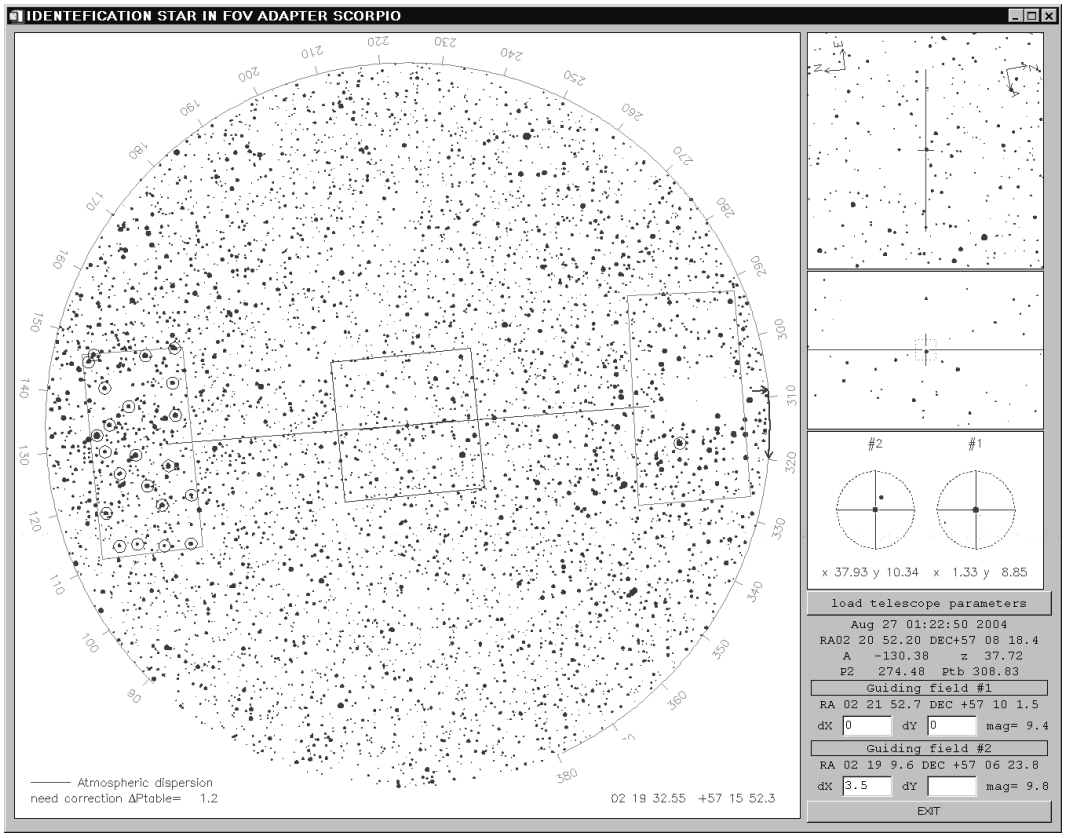

Figure 8: *Menu of the guiding stars search program. Right fields (from top to bottom) – the SCORPIO field of view where slit position is marked, fields of view of TV viewing system in the modes of pointing and guiding. The rectangles in the large left field mark the displacement range for the guiding fields (last are marked by the circles.*

Table 3: *Parameters of the CCDs*

	The detector	
	TK1024	EEV-42-40
Type	Thin, back-illuminated	
Size	1024 × 1024	2048 × 2048
Size with overscan	1034 × 1034	2068 × 2072
Pixel size, μm	24	13.5
Scale[1], $''$/px	0.32	0.18
Field of view[1], arcmin	5.4	6.1
Max DQE, %	80	83
Gain, ē/ADU	1.3	0.50–2.07
Readout noise, ē	3	1.8-4
Dark current, ē/min	0.1	0.03

[1] Till September 2003 the optics supported the focal ratio $F/2.9$ was used. In this case the scale on CCD TK1024 was $0.28''$/px, with the field of view $4.8'$

Table 4: *Structure of the broad-band filters*

Filter	The mark and thickness of the glasses
U	UFS-6 (1.0 mm) + SZS-21 (3.0 mm)
B	CC-5 (1.5 mm) + SZS-22 (2.5 mm)
V	SZS-22 (1.0)+ ZHS-18 (3.0 mm)
R_c	SZS-27 (2 mm) + OS-13 (3 mm)
I_c	FS-6 (2.0 mm) + KS-15 (2.0 mm)

It is recommended to carry out observations of stars – spectrophotometric standards in the mode of slitless spectroscopy. In so doing, to isolate an object in the center of the field of view, a circular mask is used, which is generally mounted in position "5" of Wheel 2. It provides a non-vignetting field of view about $30''$ in diameter.

3.2. Filters

All filters used in the SCORPIO are equipped with bayonet holders with an inner diameter of 72 mm, which enable the filters to be readily changed in the wheels by means of a special filter demounter. Speaking below of the diameter of filters we will bear in

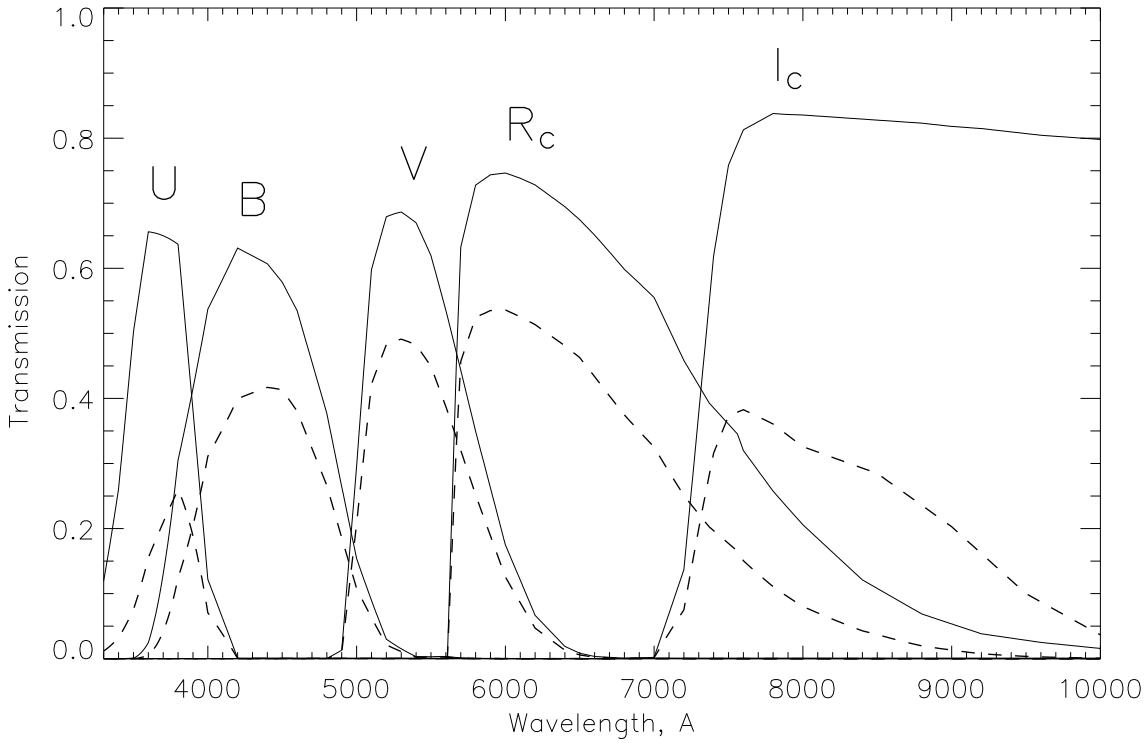

Figure 9: *Spectral transmission curves of the glass filters (the solid lines). The dotted lines indicate the curves if the transmission of SCOPRIO optics and the CCD EEV-42-40 sensitivity curve were taken into account.*

mind their light (inner) diameter which is smaller than that of the holder.

3.2.1. Broad-band filters

Glass broad-band filters are employed for construction of Johnson-Cousins photometric system ($UBVR_cI_c$) in the mode of direct imaging. The diamter of the filters is 70 mm, the thickness is 4–5 mm. Theoretical transmission curves where quantum efficiency of the the SCORPIO optics and CCD were taken in account are shown in Fig.9. The properties of the colored optical glass from which the filters are composed (mark of the glass and its thickness) are presented in Table 4. As a rule, the filters BVR_cI_c are permanently mounted on Wheel 2.

3.2.2. Medium-band filters

The set of medium-band interference filters of diameter 72 mm with a bandwidth $FWHM = 160 - 400$Å was produced in Research Institute of Precision Devices (Moscow). In the mode of direct imaging these filters can be applied to executing different tasks, such as construction of spectral energy distribution (SED) for faint objects or observation of extended objects in different emission lines and in the continuum. I.D. Karachentsev put at our disposal a 50-mm filter with a bandwidth $FWHM = 75$Å (FN657), centered on the non-redshifted H_α line, which is now used for mapping of the ionized gas distribution in galactic nebulae and nearby galaxies. Interference filters need to be mounted on Wheel 1 (at the focal plane of the telescope) for avoiding variations of the central wavelength over the field, which are associated with the change of the angle of light incidence on the filters in the Wheel 2.

The spectral transmission curves of the filters, measured with the spectrograph MPFS at the direct focus of BTA (i.e. in a convergent beam $F/4$) are shown in Fig.10, their main characteristics are listed in Table 5. Unfortunately, MPFS fails to measure the curves for two bluest filters (SED345 and SED375), in this case table presents only maker's characteristics measured by the manufacturer for the case of normal incidence of rays on the surface of the filters.

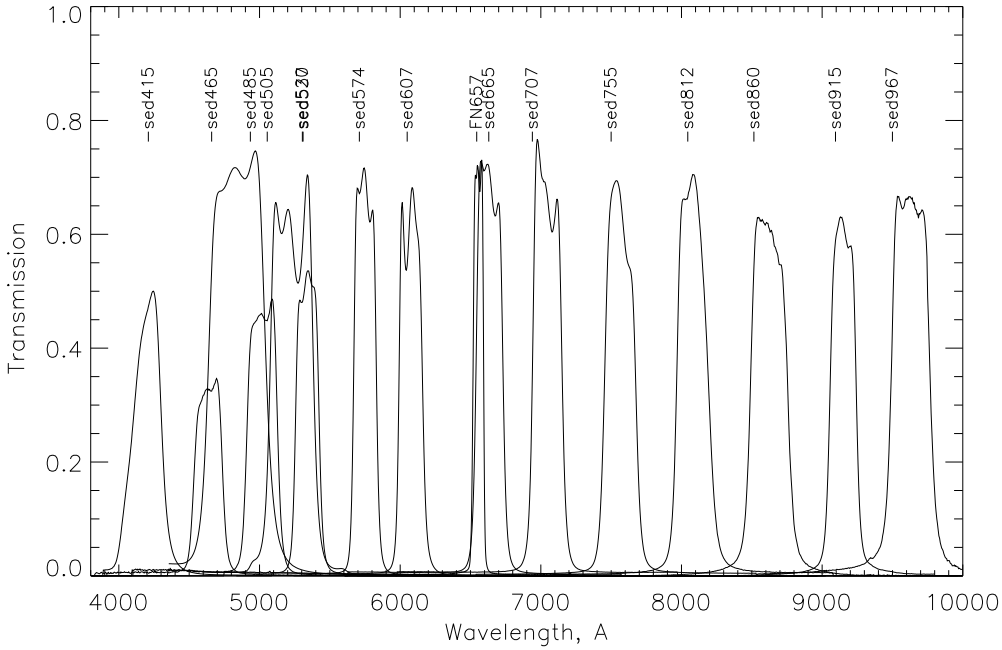

Figure 10: *Spectral transmission curves for the medium-band filters.*

Table 5: *Properties of the medium-band filters*

Filter	T_{max}, %	λ_c, Å	FWHM, Å
SED345	60	3450	420
SED375	75	3760	300
SED415	50	4200	212
SED465	35	4620	205
SED485	75	4850	409
SED505	49	4990	221
SED520	70	5230	310
SED537	54	5310	168
SED574	72	5730	161
SED607	68	6060	167
SED665	73	6620	190
FN657	73	6555	75
SED707	77	7040	207
SED755	69	7560	220
SED812	71	8090	222
SED860	63	8620	269
SED915	63	9150	188
SED967	67	9616	280

3.2.3. Narrow-band (IFP) filters

The narrow-band filters with a bandwidth $FWHM = 10 - 20$ Å are used in observations with the Fabry-Perot interferometer to isolate the required spectral range. Observations of galaxies require a set of filters centered on the redshifted emission lines. At present the SCORPIO is equipped with several sets of such filters.

In Research Institute of Precision Devices (Moscow) filters 55 mm in diameter were made, which can be used in observations around the line [OIII]λ5007 ("green") and near the lines H_α, [NII]λ6548/6583, [SII]λ6716/6731 ("red"). The spectral transmission curves of these filters, measured with the spectrograph MPFS at the direct focus of BTA (in a convergent beam $F/4$) are presented in Figs. 11–12, their main characteristics are given in Table 6. The specification of the filters begins with "IFP".

50-mm filters (denoted as #76B ... #81B) for observations around the H_α line are made available to us by our colleagues from Byurakan AO (Armenia). The filters were made by the company Barr Associates Inc. (USA) at the request of Marseille Observatory (France). The spectral transmission curves and characteristics of the filters measured in Marseille Observatory and recalculated by us for the case of observations in the beam $F/4$ are presented in Fig. 12 and Table 6.

7 filters of diameter 50 mm (designated as AC6700...AC6790) for observations around the H_α line produced by Andover Corporation (USA), were given by J. Barbiery (Padova University, Italy). The makers' data (curves of transmission and character-

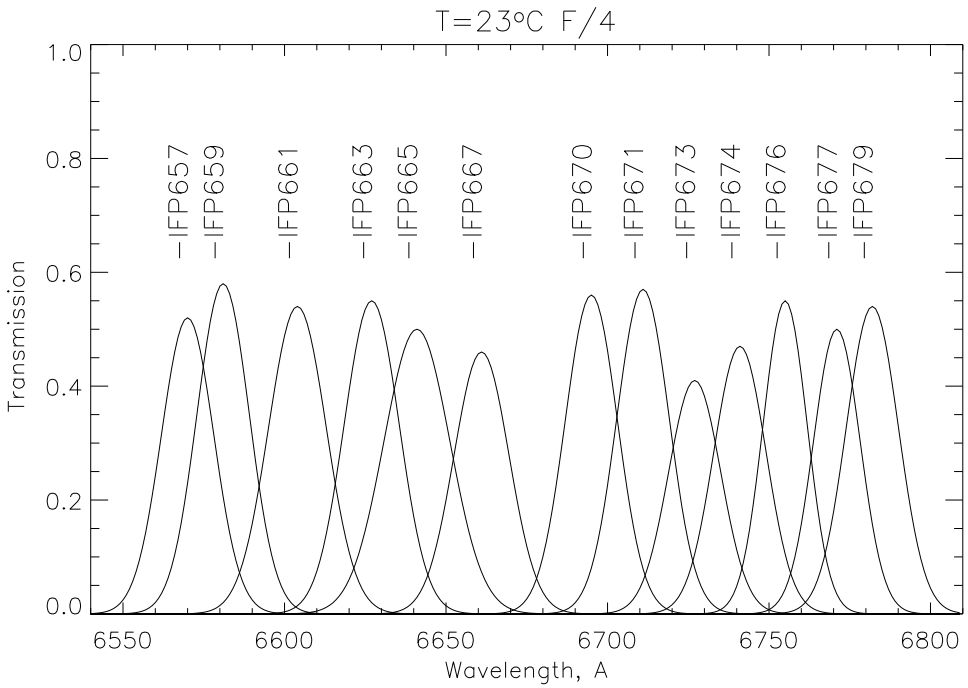

Figure 11: *Spectral transmission curves for the "red" IFP-filters.*

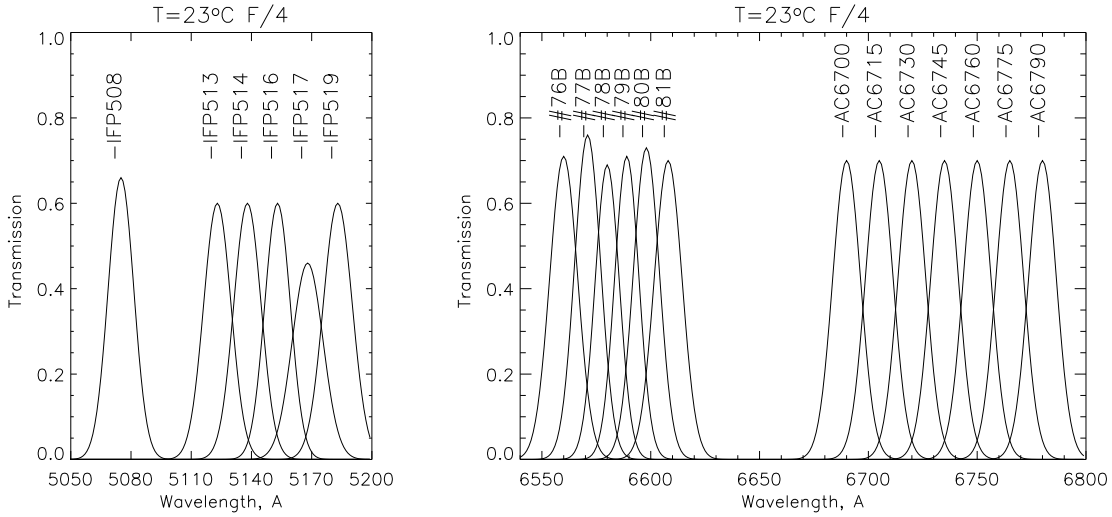

Figure 12: *Spectral transmission curves for the "green" IFP-filters (left) and "red" IFP-filters produced by Andover Corporation, and filters from Byurakan AO (right).*

istics of the filters) recalculated by us for the case of observations in the beam $F/4$ are given in Fig. 12 and Table 6.

Objects with velocities from -200 to $+10\,000\,kms^{-1}$ in the line H_α and from $+3\,500$ to $+11\,000\,kms^{-1}$ in the line [OIII]λ5007 can be observed with the filters described above.

It should be noted that the values of the central wavelength of the interference filters (λ_c) changed linearly with temperature: $\Delta\lambda_c \approx 0.15 * \Delta T$.

3.3. Grisms

The SCORPIO is equipped with a set of the transparent grisms (which are a combination of a transparent diffarction grating and 2 prisms). The grisms

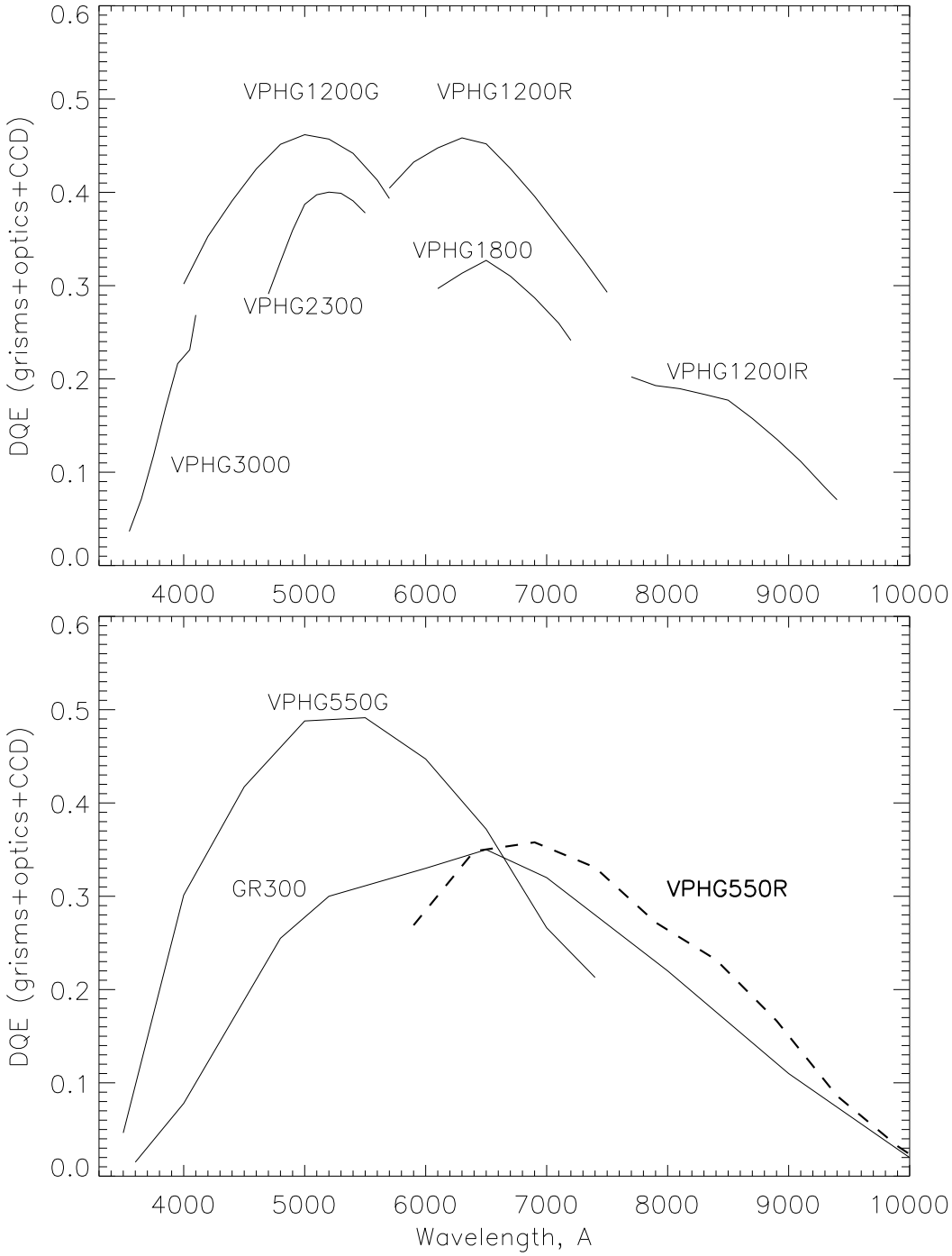

Figure 13: *The theoretical quantum efficiency curves for spectral observations with different grisms. The transmission of SCOPRIO optics and the CCD EEV-42-40 sensitivity curve were taken in account.*

are mounted on the carriage of dispersing units in position "0" on wedge-like guides. The holders of the grisms enables their rotation around the optical axis since in the "long-slit" mode the dispersion direction must coincide with the X-axis on the CCD chip, whereas in the mode of multi-slit spectroscopy it must be directed along the Y-axis (the slit in Wheel 1 is perpendicular to all the slits in the multi-slit unit because of design features of the device).

The main parameters of the grisms are listed in Table 7. Here the specification "GR" marks transparent gratings with a surface relief, representing replicas

Table 6: *Properties of the narrow-band filters (for T= 23° C, F/4)*

Filter	T_{max}, %	λ_c, Å	FWHM, Å
IFP508	66	5075	15
IFP513	60	5123	16
IFP514	60	5138	16
IFP516	60	5153	15
IFP517	46	5168	18
IFP519	60	5183	17
IFP657	52	6570	19
IFP659	58	6581	19
IFP661	54	6604	21
IFP663	55	6627	20
IFP665	50	6641	24
IFP667	46	6661	20
IFP670	56	6695	19
IFP671	57	6711	19
IFP673	41	6727	19
IFP674	47	6741	19
IFP676	55	6755	16
IFP677	50	6771	17
IFP679	54	6782	19
#76B	71	6560	15
#77B	76	6571	14
#78B	69	6580	13
#79B	71	6589	13
#80B	73	6598	14
#81B	70	6608	15
AC6700	60	6690	15
AC6715	60	6705	15
AC6730	60	6720	15
AC6745	60	6735	15
AC6760	60	6750	15
AC6775	60	6765	15
AC6790	60	6780	15

from grooved gratings produced in Vavilov State Optical Institute (GOI) (St. Petersburg). The specification "VPHG" designates volume-phase holographic gratings, which have high percentage of transmission and a low level of scattered light (Barden et al. 2000). The main set of such gratings was manufactured by the company Wasatch Photonics (USA, http://wasatchphotonics.com") at the request of the Institute of Astronomy RAS (Moscow) and given to SAO within the framework of cooperative investigations. The gratings VPHG1720 and VPHG2310 were placed at our disposal by Padova University (Italy). The curves of quantum efficiency of the SCORPIO in the spectral mode are displayed in Fig. 13.

3.4. Scanning IFP

The scanning piezo-tuned interferometer Fabry-Perot ET-50 is mounted on the dispersers' unit in position "1". There are two IFP at SAO which were given for use by Marseille Observatory (France) and Byurakan Observatory (Armenia). The parameters of the used IFPs are given in Table 8. According to our estimates, the total quantum efficiency of the SCORPIO in obeservations with IFP (telescope+reducer+filter+IFP+CCD) is about 20% in the region of H_α.

Observations with the IFP consist in sequential obtaining several dozen images of interference rings from an emitting object (or a calibration lamp) when an optical path between the plates of the IFP is changing. The radius of the rings is a function of wavelength and distance between the parallel plates of the interferometer. The full set of such images filling an interfringe is named a cycle of scanning, one image is called a channel. Control of the scanning (change of the distance between parallel reflectingv plates) is executed by means of a special controller Queensgate CS-100, connected with a personal computer. The number of spectral channels (n_z) is not rigidly regimented and may be chosen by users. Usually 32 channels are used when working with IFP FP260 and 36 channles in observations with FP500 since the number of channels must be 2–3 times larger than the finesse of the IFP.

4. System of remote control

4.1. General description

The control system of the SCORPIO incorporates remote control of the following independent units:

1. Focal reducer. The remote control is executed by the following devices:

   - Two filter wheels. The rotation is performed by a step motor, in each wheel there are two microswitches. The first one operates when the wheel is set in position "0", the second one operates when the wheel is placed in any of 6 fixed positions (fixation of positions is mechanical).
   - Mechanism of focusing of the collimator, which consists of a step motor and two microswitches at the limits of focusing. The setting of the required value of the focus in mm is performed from the number of steps passed from microswitches.
   - Mechanism of the dispersers input/output. It includes a dc-motor and two microswitches at each of the fixed positions.

Table 7: *The parameters of the grisms*

Name	grooves/mm	Sp. range[1] $\lambda_1 - \lambda_c - \lambda_2$, Å	recip. dispersion[2] Å/px	Sp. REsolution $\delta\lambda$, Å
GR300	300	3500-6500-9500	3.5	20
GR300G	300	3500-6500-9500	3.5	20
GR300R	300	5500-8000-10000	3.5	20
GR600G	600	3700-5400-7200	1.7	10
GR600R	600	6600-8300-10000	1.7	10
GR1200G	1200	4200-5050-5900	0.85	5.0
VPHG550G	550	3100-5100-7300	2.1	10
VPHG550R	550	5900-8000-10100	2.1	10
VPHG1200G	1200	3900-4800-5700	0.88	5
VPHG1200R	1200	5700-6500-7400	0.86	5
VPHG1720	1720	6250-6750-7250	0.50	2.5
VPHG1800R	1800	6100-6580-7100	0.52	2.5
VPHG2300G	2300	4800-5150-5600	0.38	2.2
VPHG2310	2310	4800-5200-5600	0.35	2.2
VPHG3000B	3000	3500-3800-4100	0.20	1.5

[1] λ_c – the central wavelength

[2] For CCD EEV-42-40 in the center of the chip

Table 8: *Scanning Fabry-Perot interferometers*

	The interferometer	
	FP260	FP500
order of an interference[1]	235	501
spectral resolution, $\delta\lambda$[1]	2.5 Å	0.7 Å
spectral range, $\Delta\lambda$[1]	29Å	13Å
Finnese $F^1 = \Delta\lambda/\delta\lambda$	11	17
number of spectral channels n_z	$24 \div 32$	$32 \div 40$

[1] at the wavelength 6563 Å

• Mechanism for input/output of the polarization analyzer, including a step motor and two microswitches.

• On/Off switch of the electromagnetic shutter.

• Readout of the temperature from the thermal sensor placed on the control board.

2. The prime focus platform-adapter. The remote control here is implemented by the following devices:

• Step motor which sets the diagonal mirror in two positions. In the position "Field" the mirror is placed in the beam and reflects the image of the field of view to the TV viewing system and also reflects light from the calibration lamps to the reducer. In the position "Fibers" the mirror is removed from the beam and sends images of the guiding stars to the TV. The movements of the mirror is limited by the microswitches.

• Motors of the guiding fields "1" and "2". Each bundle of fibers is moved by two steppers on the coordinates "X" and "Y". The limits of the movements of the motors have microswitches.

• Step motor of focusing the image in fiber "2", the limits of the movements of which are provided with microswitches. The focus position in the middle between microswitches is adopted to be "0".

• Three LEDs illuminating the crosses (two in the fiber bundles and one in the field). The brightness of illumination changes discretely (256 levels of brightness).

• Switching On/Off of the electromagnetic shutter.

• Switching On/Off of the calibration lamps NEON and FLAT.

3. Mutlislit unit. The remote control here is exe-

cuted by the following devices:

- Step motor insert/removal of the multi-slit unit from the light beam. The limits of movements of the stepper have microswitches.
- Step motor of the frame with catching magnets. The limits of movements of the motor have microswitches.
- Switching On/Off of 16 catching and 16 holding electromagnets, and also one double electromagnet for holding all the slits. Small (separate for each slit) catching and holding magnets are used only for placing the slits in the required positions. Then they are switched off and the big magnets hold all slits. Such a scheme is used for the purpose of saving small magnets from premature fuse out.

4. Controller of modes of the CCD.
5. Controller of the scanning IFP.

4.2. Controller of microprocessors of the SCORPIO

The first three above-enumerated devices (the reducer, the adapter and the multi-slit unit) incorporate electronic boards on each of them a microprocessor is mounted. These boards (subsequently named the SCORPIO-1, SCORPIO-2, and SCORPIO-3) control following electromechanical devices:

- SCORPIO-1: 4 steppers and 1 dc-motor, 10 microswitches, the thermosensor.
- SCORPIO-2: 6 steppers and 12 microswitches, a shutter, 2 lamps, 3 LEDs with 256 gradations of brightness.
- SCORPIO-3: 2 steppers and 4 microswitches, 33 electromagnets.

The adopted design in which every unit of the SCORPIO has an independent control board possesses the advantage that these modules can operate as part of other devices of BTA. Such realization of remote control of the device makes it possible to reach the desired stability in the operation throught the existing long lines of communication with the 6 m telescope prime focus. There is no need of continuous control of the motors, because these functions are executed by micropocessor. At the same time, there is no necessity for the re-programming of the microprocessor for any possible changes of the procedure of observations and software on the control computer. Both the shutters and the lamps can also be controlled directly from the controller of the CCD and also from switches on the casing of the reducer and the adapter.

All three boards are connected sequentially to the serial port of the control computer (by the interface RS232) through a small board-commutator mounted inside the platform-adapter.

4.3. Control of CCD

The controller of the CCD is installed in the prime focus cabin. Besides the control of the CCD itself, the controller operates the shutter of the SCORPIO. To operate with the controller of the CCD EEV-42-40, the acquisition software DINA, developed in the Laboratory of Advanced Design of SAO RAS, is used. This software sets the modes of operation of the controller, performs acquisition frames from the CCD, visualizes them and writes images in standard FITS format.

4.4. Control of the Fabry-Perot interferometer

The scanning Fabry-Perot interferometer ET-50 produced by Queensgate is operated by the controller CS100. The piezoelectric actuators connected to the controller change the gap between the two reflecting plates of the interferometer. The parallelism of the plates is supported by the sensitive capacitance micrometers sending feedback signal to the CS100 controller. The interferometer ensures normal operation in a temperature range from 0 to 50 °.

During observations the controller is near the IFP and is connected to it through special sealed connectors by a flexible multicore cable to 3 meters long. The serial-port interface permits the control computer and the working place of an observer to be located at a distance of several hundred meters away from the telescope. The controller stabilizes effectively the parameters of the IFP and allows control of scanning through a computer serial port via standard RS232 interface.

5. Characteristics of observations in different modes

5.1. Modes of observations

Table 9 presents positions of the main elements of the SCORPIO in different modes of observations (the numbers of the positions are in brackets). Since in changing the modes different optical elements are placed in the beam, then the position of the focal plane at the exit of the reducer may be shifted. The compensation of these displacements is performed by means of changing the position of the focus of the collimator. In the SCORPIO the reference position is such a focus value at which the focal plane of the collimator coincides with the position of the slit of the

Table 9: *The modes of observations with the SCORPIO*

Name of the mode	MODE[1]	The positions of the movable elements				
		Wheel 1	Wheel 2	Disperser	Multislit	analyzer
Direct images	Images	("0"..."5")	("0"..."4")	Hole ("0", "1")	–	–
Interferometer F-P	IFP	("1"..."5")	("0")	IFP ("1")	–	–
Long-slit	Spectra	slit ("3")	("0")	grism ("0")	–	–
Slitless spectroscopy	Spectra	"0"	mask ("5")	grism ("0")	–	–
Multislit spectroscopy	SpectraMUL	"0"	"0"	grism ("0")	in beam	–
Spectropolarimetry	SpectraPOL	dash ("5")	"0"	grism ("0")	–	in beam
Polarimetry in filters	ImagesPOL	("0"..."5")	("0"..."5")	Hole ("0", "1")	–	in beam

[1] The name of a descriptor in a FITS-header

spectrograph, under the condition that the movable elements (analyzer, filters, etc.) are removed from the beam (excluding the long-slit in Wheel 1). Before the observations, it is necessary to focus the collimator by the image of the slit, illuminated by the calibration lamps NEON or FLAT. The measured value of the reference focus of the collimator (F_{slit}) is included into the parameters of the spectrograph control program. In changing the mode of observations, this program automatically changes the value of the collimator current focus. The required value of the focus (F_{col}) can be computed by the formula:

$$F_{col} = F_{slit} - \Delta F_1 - \Delta F_2 - \Delta F_{polar} + \Delta F_{disp},$$

where ΔF_1, ΔF_2 are the corrections of the focus for the filters in Wheels 1 and 2 determined in the general form by the relationship $\Delta F = h(n-1)/n$, where h is the thickness and n is the mean index of refraction of the material of the filter.

ΔF_{disp} is the correction for the dispersing element, the correction is equal to 0.3 mm for the grism[3], -0.1 mm for the IFP 260 and $+0.2$ mm for IFP 501.

ΔF_{polar}=5 mm is the correction for the input of the polarization analyzer.

When observing with the multi-slit block, the value F_{multi} is taken as the reference focus, which corresponds to the position of the best focus in focusing by the image of the multi-slit block itself (when other optical elements are removed from the beam). Because of the design peculiarities $F_{multi} \approx F_{slit}+3$ mm.

[3] The correction is caused by the distinction between best focus value measured on the slit image and one on the spectral lines.

5.2. Calibration frames

When observing with the SCORPIO, the following calibration frames are used.

- BIAS – readout of the CCD with a zero exposure. Usually a series of 10–20 such exposures starts at the beginning and at the end of the observation night in order to average them.
- DARK – frame of "dark current". Generally, this calibration is not used in observations with the CCD EEV-42-40 which has no hot columns and the level of dark current is low. However DARK frames are necessary if, for technical reasons, observations have to be made with a detector having worse characteristics. Then it is necessary before (or after) the observations to expose a series of dark frames of the same length as the exposure of an object and form a medium frame.
- NEON – calibration of the scale of wavelengths. It is necessary in all spectral modes and in observations with the IFP. It is executed with the aid of a He-Ne-Ar–filled lamp placed on the platform-adapter. With the aim of taking account of the internal flexures of the instrument, it is needed to expose an individual NEON frame, if the change of the zenith distance is over $10-20°$.

In observations with the IFP it is necessary to expose a whole cube of the data (all the channels of the interferometer) with images of interference rings from the line of calibration spectra cut out by a narrow filter. The calibration cube needs to be exposed at least twice a night (before and after the observations). In the course of scanning of an object 4–6 exposures of NEON in different channels of the interferometer should be made. These frames are used in the reduction of observational data to check the positions of the center of the rings and the accuracy of scanning

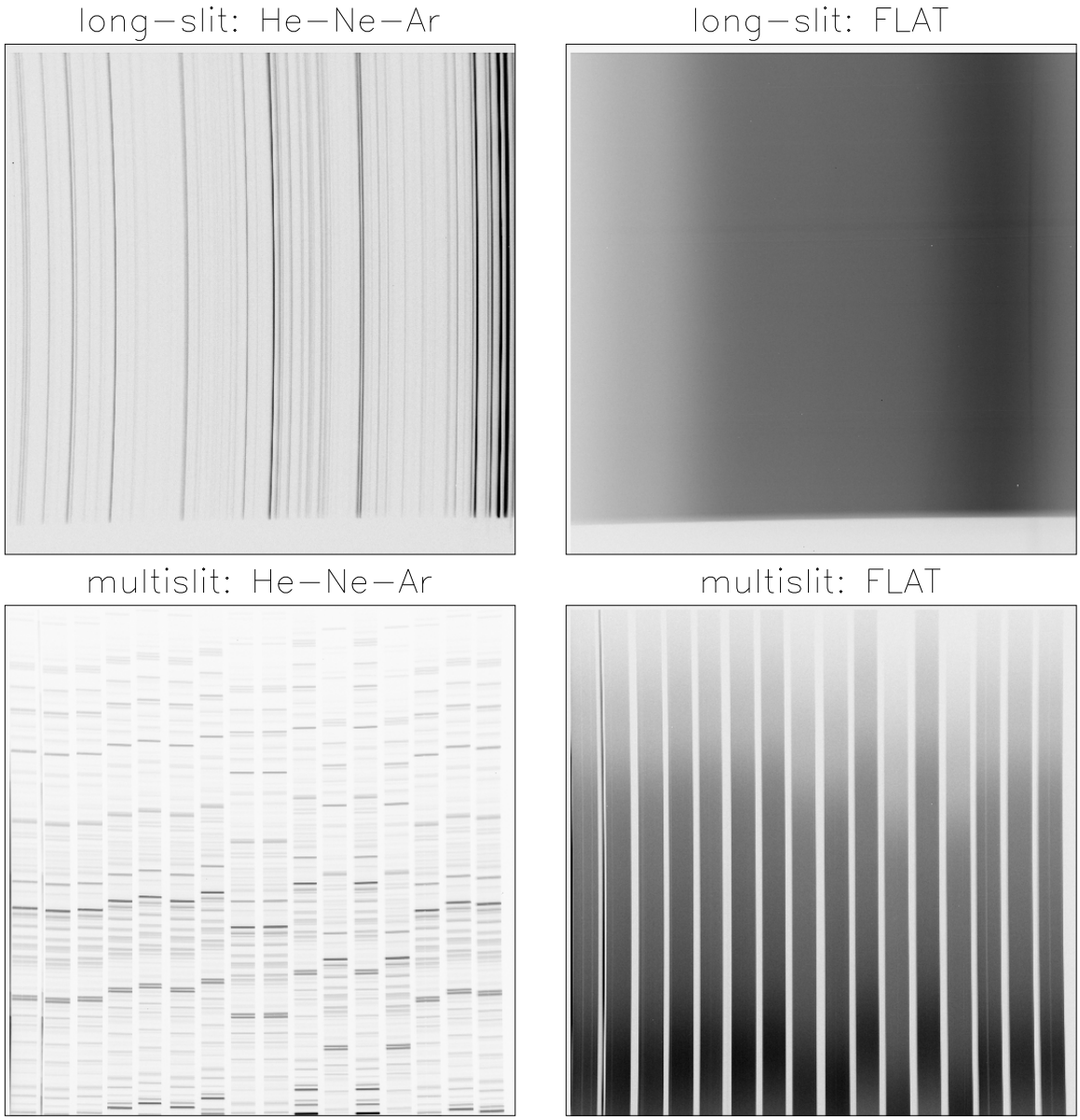

Figure 14: *The raw calibration frames of a He-Ne-Ar lamp (left) and a flat-field lamp (right). The modes of long-slit (top) and the multi-slit spectroscopy (bottom). A dispersion direction in these modes is different (from left to right and from top to bottom respectively), because of constructive peculiarities of the device.*

of the IFP.

• FLAT – calibration of homogeneous lighting of the flat field from a continuous spectrum lamp. It is necessary in all modes, it is executed at the beginning and end of the observations in the case of direct imaging and observations with the IFP, and several times during the night in spectral observations at different zenith distances. In the case of IFP these are exposures of the homogeneous lighting of a narrow filter in each IFP channels, in the case of spectral observations these are the exposures of the continuous spectra, in the case of direct imaging — the frames of homogeneous lighting (twilight sky or lamp FLAT) in the desired filter.

Examples of spectral frames of both calibration lamps for different conditions of observations are shown in Figs. 14 and 15.

5.3. Direct images

As has already been noted in Chapter 3.2, the SCORPIO is equipped with a few sets of filters which

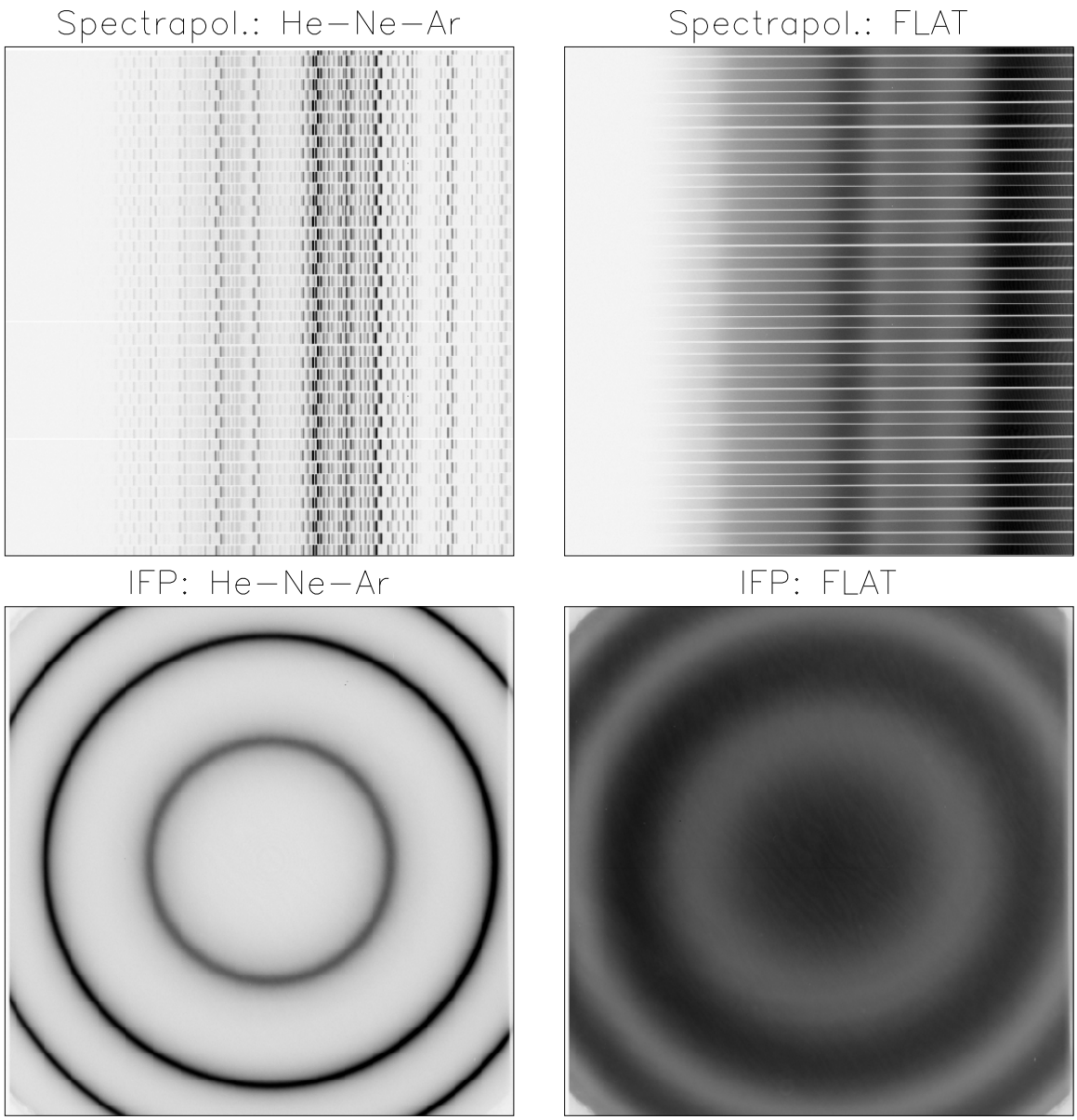

Figure 15: *Raw calibration frames of the He-Ne-Ar lamp (left) and the flat-field lamp (right). Top – the mode of spectropolarimetric observations with a dashed slit, a shift of the wavelength scale between different polarized beams is visible. The dispersion direction is from left to right. Bottom – the mode of IFP, here the dispersion is directed to the center along the radius.*

can be used for photometric observations. Glass broad-band filters are employed for construction in the direct imaging mode the photometric system $UBVR_cI_c$ of Johnson-Cousins (see Bessell 1990). Table 10 presents limiting magnitudes for the detection of faint objects at a level of signal/noise=3 with a seeing of $1.3''$. The table is computed on the basis of the paper by Fatkhullin (2002) in which capabilities of the SCORPIO (with CCD TK1024) from photometry of faint starlike and extended objects were investigated.

Table 10: *The limiting magnitudes in broad-band filters (Fatkhullin 2002)*

Filter	T_{exp}	mags
B	2500	27.0^m
V	1500	26.3^m
R_C	1260	26.4^m
I_C	1800	25.1^m

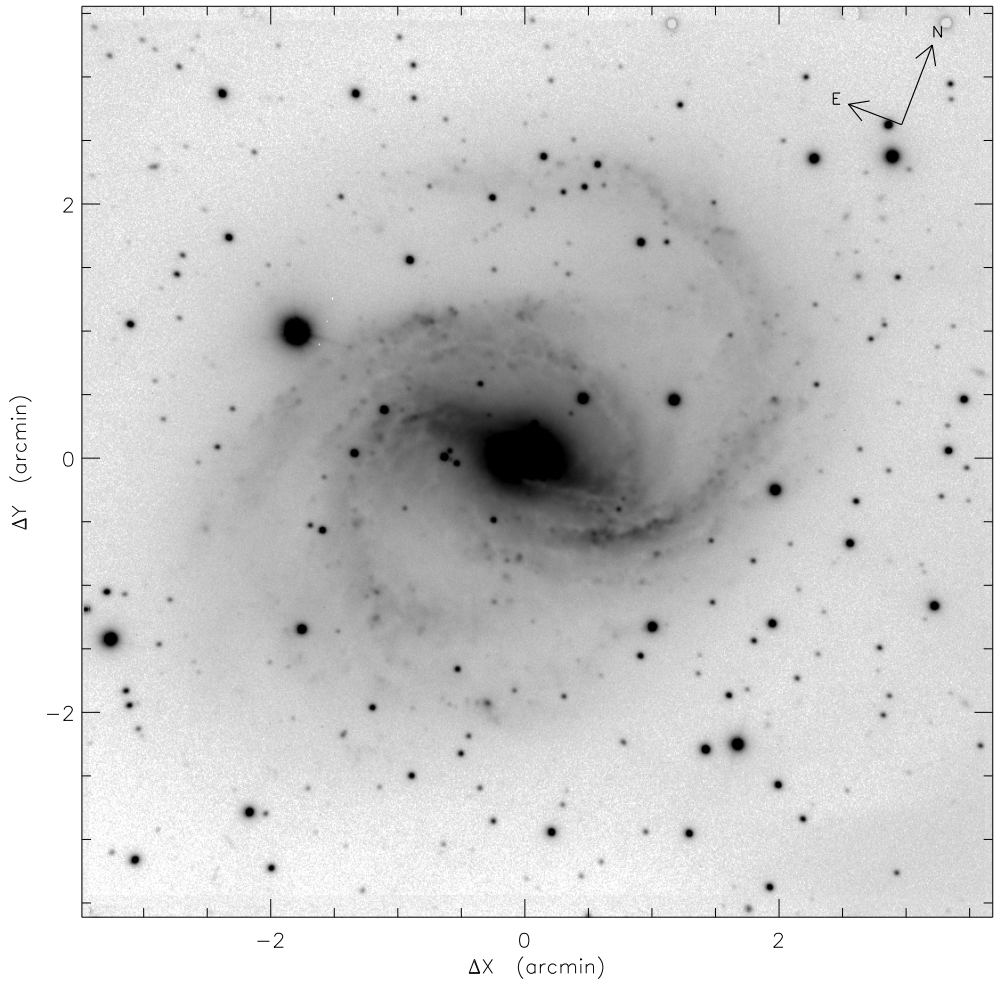

Figure 16: *Image of the galaxy NGC 6951 obtained with the SCORPIO in the filter* R_C. *The seeing is* $1.4''$, $T_{exp} = 90$ *s.*

Medium-band interference filters can be employed for the construction of the spectral energy distribution of faint objects in the field, or for obtaining images of extended objects in different emission lines (H_α, [OIII] etc.) and in the continuum.

The relatively high focal ratio of the device makes the SCORPIO an efficient instrument for photometry of extended objects. An image of the nearby galaxy NGC 6951 is shown in Fig. 16. The level of surface brightness of external isophote of $23.4^m/\square''$ in filter R_c is reached here during an exposure of a minute and a half only.

The basic problem of photometric observations is the interference pattern (fringes) when observing in the "red" photometric bands (see Chapter 6). Thus, in observations in filter I_c with CCD EEV-42-40 the level of fringes reaches 8% of the sky background.

5.4. Long-slit and slitless spectroscopy

The preimaging possibility proves to be very useful in slit spectroscopy of both extended objects (since the slit position is known exactly) and starlike objects if the latter are too faint to be visible on the TV-viewing system. Thus, for example, a 1–2 minutes trial exposure in the filter R_c is sufficient for reliable pointing to objects of $22–23^m$ at a moderate seeing. In the pointing process, an image of the object under study is set on the detector where the slit image is projected. Subsequently, the slit is set in place of the filter, and a grism is inserted in the collimated beam, which turns the focal reducer into a fast spectrograph. The change of the "direct imaging"–"long slit" configurations takes about one minute.

Fig. 17 shows sequentially the process of obtaining

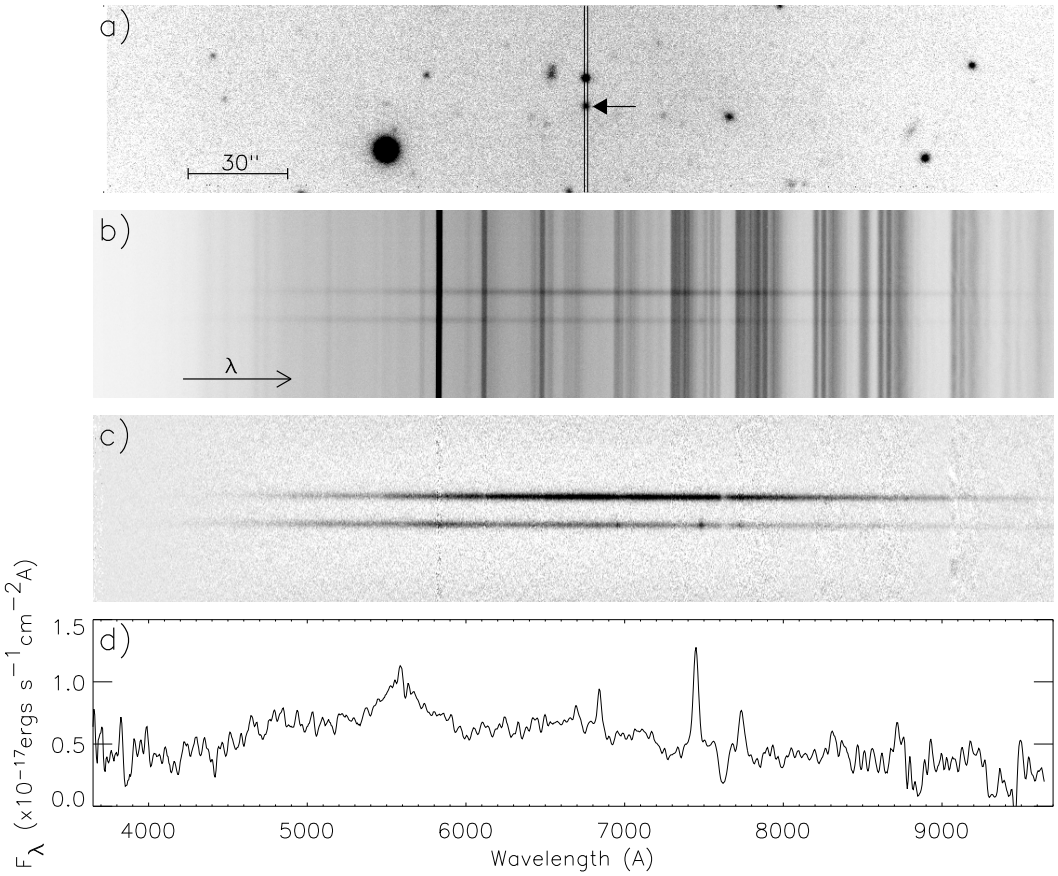

Figure 17: *Spectroscopy of the radio galaxy RCJ 1154+0431 with the SCORPIO: (a) a fragment of R_C (T_{exp} = 60 s) image, the position of the spectrograph slit is shown, the radio galaxy is marked by the arrow; (b) a low-resolution spectrum (the sum of two 600-s exposures); (c) the same after the subtraction of the night-sky spectrum; (d) the integrated spectrum on the wavelength scale.*

observational data using the spectroscopy of the radio galaxy RCJ1154+0431 (observations made at the request of Yu.N.Parijskij). The total V magnitude is 19.8^m, its measured redshift is z=1.0 (see Afanasiev et al. 2003).

The SCORPIO is equipped with set of grisms ensuring observations with different spectral resolution (from 1.5 to 20Å with a slit width of 1″) in different regions of the optical spectrum. Up to 2003 observations were made with the aid of transparent grids with profiled grooves, the density of the grooves was from 300 to 1200 per mm (see Table 7). When working with such grids, the maximum quantum efficiency of the whole system (telescope+SCORPIO+CCD) was 30% for spectra of low ($\delta\lambda = 15 - 20$Å) and only 3–5% for the spectra of higher resolution ($\delta\lambda = 5 - 6$Å). In the years 2003–2004 we started observations with grisms using volume-phase holographic gratings (VPHGs), which have a higher transmission and a lower level of scattered light. Here a quantum efficiency of 20–50% is achieved both with high and low resolutions (see Fig. 13).

The achieved quantum efficiency of the instrument allowed one to continuously determine the redshifts and spectral classification of extragalactic radio sources since the required low-resolution spectra of $19 - 21^m$ objects can be obtained even at moderate atmospheric transparency and at a $3 - 5''$ seeing; the total exposure time is only 10–20 min (see, e.g., Afanasiev et al. 2003b; Amirkhanyan et al. 2004). At the same time, at a 1.5″ seeing in low-resolution spectroscopy of starlike objects, a limiting magnitude $R_c = 24^m$ was achieved over a two-hour exposure time, the signal-to-noise ratio was 10 in the continuum of the spectra obtained (Dodonov, private communication). The stability of the instrumental profile of the spectrograph, which affects both the accuracy of subtracting the night-sky lines and the possibility of allowance for the interference pattern in the detector material (see section 6), plays a crucial role in obtaining the spectra of such faint objects. The technique of displacing an object along the slit between

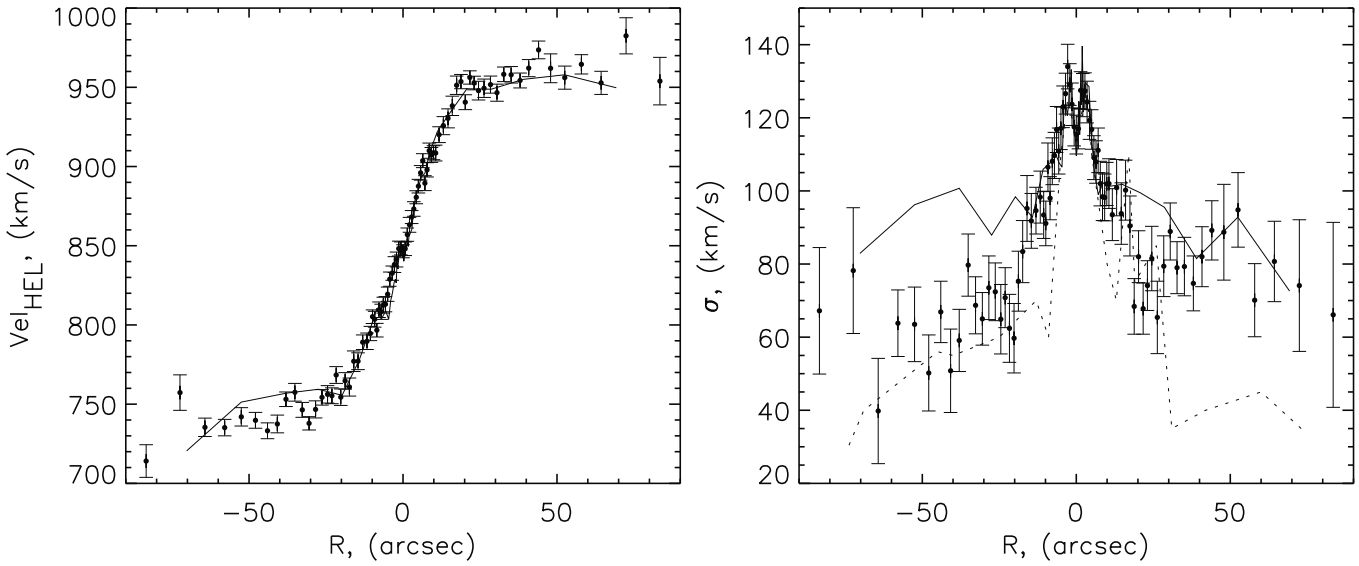

Figure 18: *Kinematics of the stellar component in the galaxy NGC 3412: the distribution of radial velocities (a) and radial-velocity dispersion (b) along the major axis. The solid and dashed lines represent the published measurements by Aguerri et al. (2003) and Neistein et al. (1999), respectively.*

exposures is of great help in such observations. During the subsequent reduction, a pure spectrum, i.e., the spectrum of the sky taken from the same location, but on the displaced frame, is subtracted from the spectrum of the object.

Investigation of the kinematics of galactic stellar disks is a good test for the capabilities of the spectrograph since absorption spectra with a relatively high signal- to-noise ratio and a spectral resolution of at least $\delta\lambda = 2 - 4$Å should be obtained here for regions with a surface brightness of $21–23^m/\square''$. Fig. 18 shows an example of measuring the parameters of the stellar kinematics along the major axis of the barred lenticular galaxy NGC 3412. Over a 1.5-h total exposure time on the SCORPIO (using VPHG2310), we can measure radial velocities and radial-velocity dispersions of stars for regions with a V-band surface brightness of $23^m/\square''$.

Slitless spectroscopy, where the slit is replaced by a circular mask about $30''$ in diameter (see Sect. 3.1), is used during the observations of spectrophotometric standard stars. This technique allows one to completely avoid the problems of light losses on the slit and distortion of the spectral energy distribution because of the effect of differential atmospheric refraction.

5.5. Multislit spectroscopy

The available set of grisms can also be used in multislit observations, although the total spectral range decreases in comparison with the long-slit case because of the slit displacement in the field. An IDL-based package of programs was written for the preliminary determination of the optimal position angle of the multi-slit unit concerning observed objects. In such observations, a direct image of the area under study is obtained, a multi-slit unit is introduced in the focal plane of the telescope, and the slits are set according to the coordinates of the chosen objects measured on the CCD array. The spectra obtained are illustrated in Figs. 14 and 19.

5.6. Panoramic spectroscopy

The scanning FPI is a highly efficient instrument for studying the kinematics of extended objects. After special reduction, the interferograms can be represented as a data cube in which two coordinate axes are located in the plane of the sky and the wavelengths (or the Doppler velocities measured from the redshifts of spectral lines) are a third coordinate. In other words, an individual spectrum is related to each image element.

There are two scanning IFP at SAO, which are described in Sect. 3.4. These are successfully used to study both Galactic (nebulae, star clusters) and extragalactic objects. For more details of the IFP observations with the SCORPIO, see Moiseev (2002). Narrow-band filters with a bandwidth of $10 - 20$Å are used to separate the required spectral range (see Sect. 3.2).

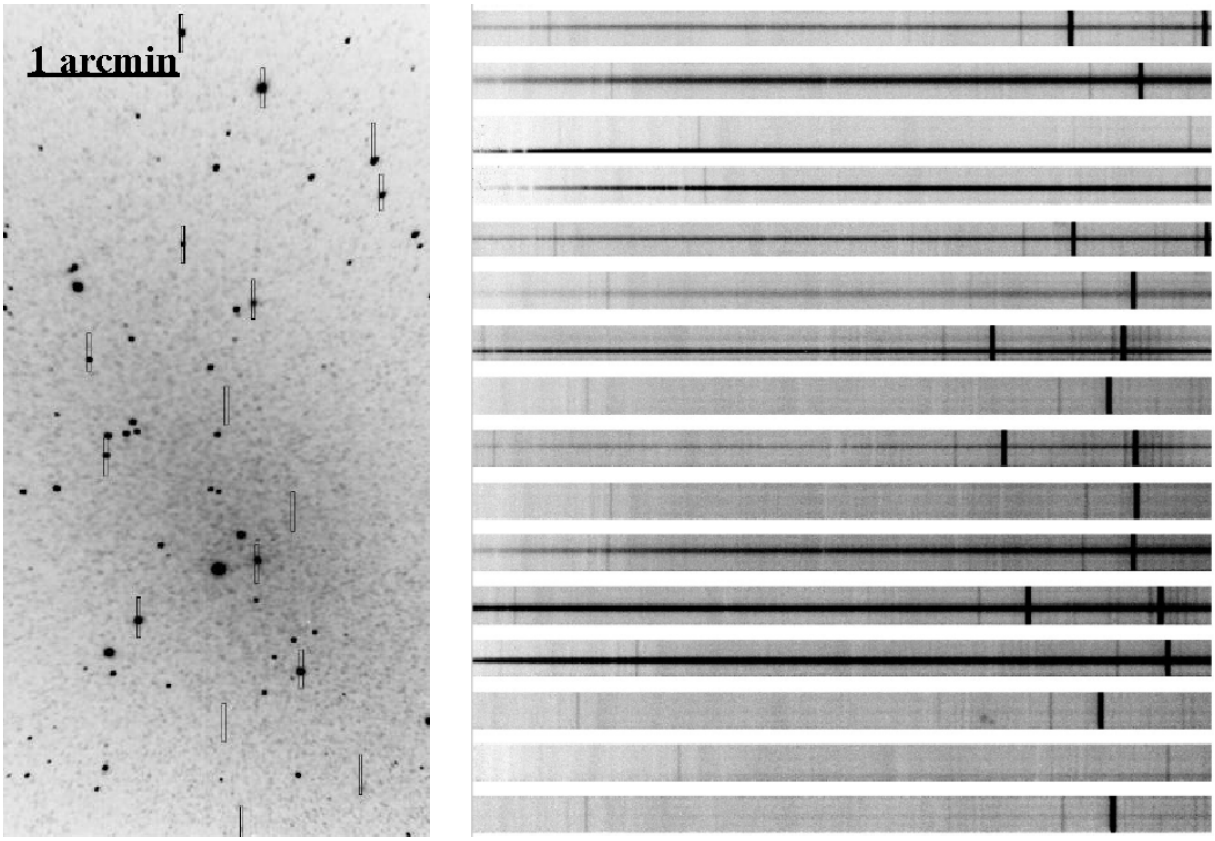

Figure 19: *Spectroscopy of globular clusters in the nearby galaxy NGC 147 (the observations at the request of M.E. Sharina): a V-band image of the galaxy with marked slit positions (left) and multi-slit spectra of the objects (right).*

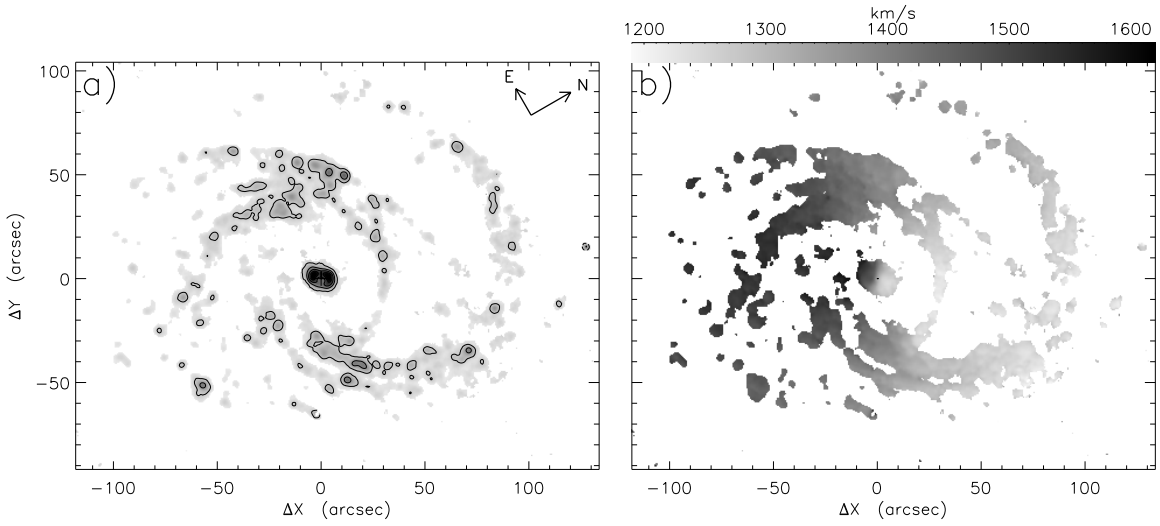

Figure 20: *Observations of the galaxy NGC 6951 with the SCORPIO in the H_α: (a) – image in the emission line, (b) – the line-of-sight velocity field.*

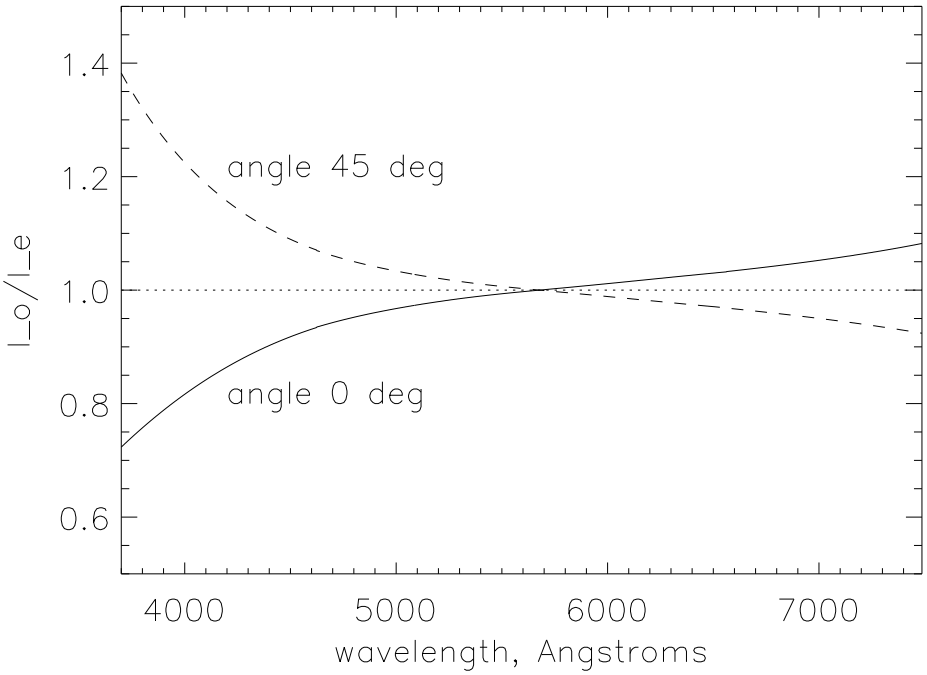

Figure 21: *Calibration curves of the relationship $R = I_o(\lambda)/I_e(\lambda)$ determined from observations of standard of zero polarization in spectropolarimetric mode of the SCORPIO for different orientations of the analyzer with the grating VPHG550.*

Table 11: *Polarization observations with the SCORPIO*

object	SCORPIO measurements		Schmidt et al.(1992)	
	P, %	θ, °	P, %	θ, °
BD+59d389	6.61 ± 0.11	97 ± 1	6.701 ± 0.015	98.09
VICyg#12	8.80 ± 0.16	117 ± 2	8.947 ± 0.088	115.03
BD+64d106	5.35 ± 0.41	86 ± 5	5.627 ± 0.037	96.63
BD+28d4211	0.33 ± 0.3	–	0.054 ± 0.030	–

Fig.20 shows the IFP observations of the nearby spiral galaxy NGC 6951. The constructed velocity field is in good agreement with similar observations by Rozas et al. (2002). Here, the radial velocities were measured with an accuracy of about $5\,kms^{-1}$.

5.7. Polarization observations

In spectropolarimetric observations, a mask that forms a dash slit is placed in front of the SCORPIO slit (see Sect. 3.1). After inserting a polarization analyzer in the beam, a series of pairs of spectra in mutually perpendicular polarization planes is obtained at the exit of the spectrograph (Fig. 15). As an alternative of $\lambda/2$-plate, we compare the spectra obtained at different orientations of the analyzer, 0 and 45°. Designate the measured intensity in the spectra at the wavelegth λ as $I_o(\lambda)$ and $I_e(\lambda)$. In an ideal instrument with zero linear polarization, the ratio $R = I_o(\lambda)/I_e(\lambda)$ by definition is equal to 1. In the real device the ratio $R \neq 1$ and depends on wavelength. This is due to the difference in the work of the grisms for the fluxes polarized in different planes. It should be noted here, that as it follows from the theory of VPH-gratings: $R(0°) = 1/R(45°)$. Fig. 21 shows an example of such a calibration relationship in which the relation $R(0°) = 1/R(45°)$ holds to an accuracy of 0.2–0.3%. After performing all the necessary calibrations (flat-fielding, wavelength-scale calibration, determination of the relation $R(\lambda)$ from the spectrum of a zero polarization standard), it is possi-

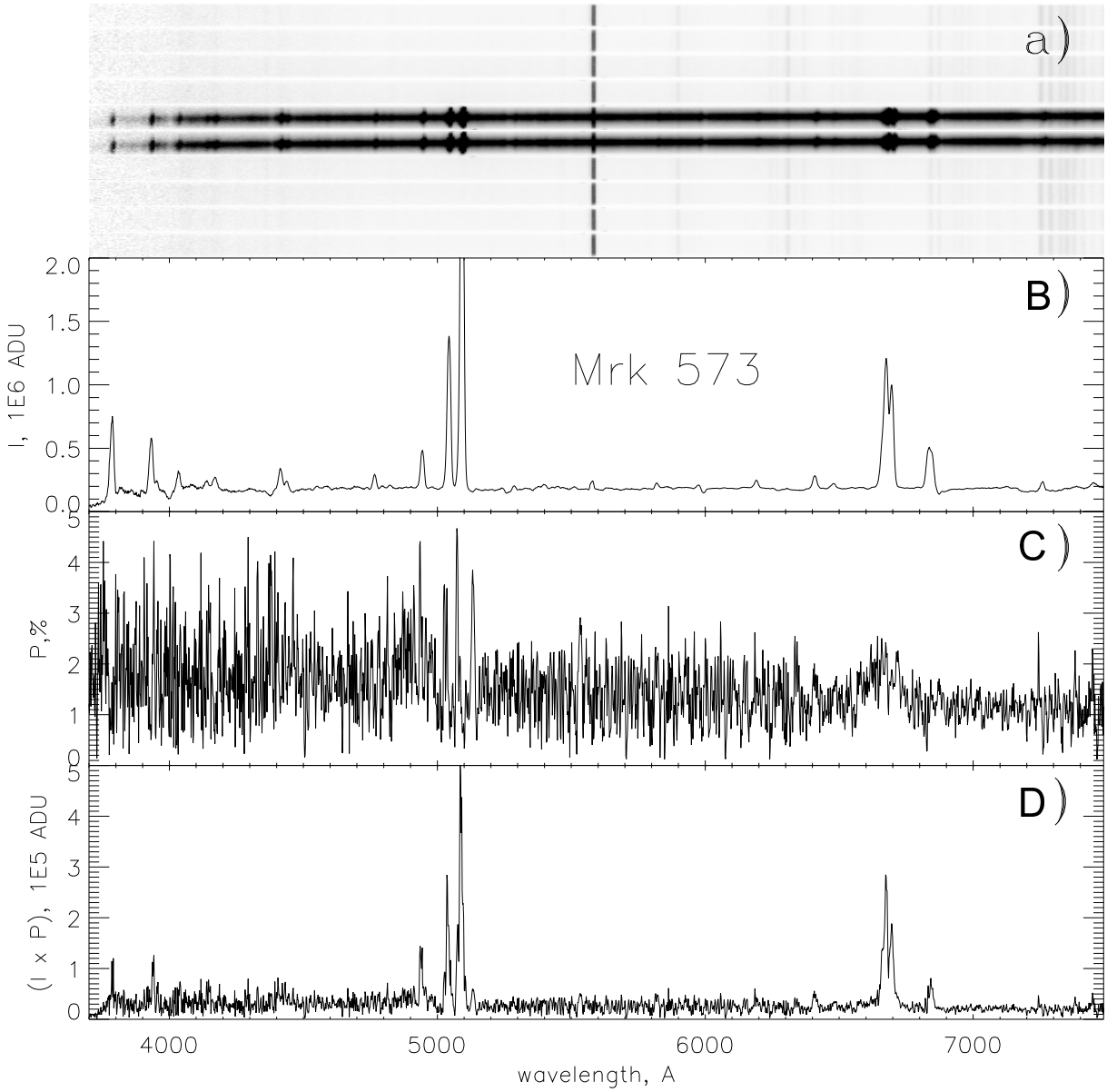

Figure 22: *Spectropolarimetry of the Seyfert 2 nucleus in the galaxy Mrk 573. The grism is VPHG550G, the exposure time is 180 min, and the slit is* $1 \times 7.5''$*: (a) the initial spectrum with the analyzer in position 0; (b) the integrated spectrum of the nucleus* ($V = 16^m$) *minus the spectrum of the surrounding galaxy (I); (c) the degree of polarization of the nucleus (P); (d) the spectrum of polarized emission* ($(I \times P)$. *ADU=0.5*$\bar{e}$.

ble to find three Stokes parameters P, U, Q from simple relationships:

$$U = \frac{I_o(\lambda)R(\lambda) - I_e(\lambda)}{I_o(\lambda)R(\lambda) + I_e(\lambda)} = P\sin(\varphi - \varphi_0),$$

$$Q = \frac{I_o(\lambda) - I_e(\lambda)R(\lambda)}{I_o(\lambda) + I_e(\lambda)R(\lambda)} = P\cos(\varphi - \varphi_0),$$

$$P = \sqrt{U^2 + Q^2}.$$

For measuring circular polarization (or the fourth Stokes parameter V) the plate $\lambda/4$ is inserted in front of the analyzer. Apart from the count statistics determined by the exposure, the actual accuracy of measuring the degree of polarization depends on the level of scattered light in the spectrograph, the accuracy of correcting the spectra for the flat field, the presence of ghosts in the analyzer (their level is about 0.2%), and the accuracy of extracting the spectra from the image.

As our observations show, the measurement threshold for the degree of linear polarization in the SCORPIO is 0.2–0.3%, and the measurement accuracy is 0.1-0.3% (depending on the exposure). Table 11 compares our measurements of polarization standards with their published data. The observed degrees of polarization were obtained by integrating the spectra obtained with the grism VPHG550G in the V band.

Fig. 22 illustrates the integrated spectrum of the central region in the Seyfert 2 galaxy Mrk 573 obtained when the SCORPIO polarization mode was tested in August, 2004. This figure shows the wavelength dependence of the degree of linear polarization. The spectra were obtained at a $2''$ seeing with VPHG550G. We took a series of 10-min exposures at successive rotation angles of the analyzer (0 and 45°). The total exposure time was 2 h, and the total V-band brightness of the galactic nucleus in the slit was about 16^m. A broad component of the hydrogen lines is distinguished in the figure. The result obtained is in satisfactory agreement with the observations of other authors (Nagao et al. 2004).

6. Data reduction

The observational data are written in the FITS format. Various standard astronomical image reduction systems, such as MIDAS or IRAF, can be used for their reduction. The primary data reduction can be easily automated, since all the necessary information about the spectrograph configuration is written in the FITS-headers. In the IDL environment, we wrote software packages for the SCORPIO data reduction and analysis. The programs for the reduction of IFP, long-slit, and multi-object spectroscopy have a user-friendly interface and can be used by users that are not familiar with the IDL language itself. The reduction sequence of FPI observations with the SCORPIO was described by Moiseev (2002).

In the reduction of observations, it is important to take into account the fringe pattern in the sensitive layer of the CCD array in the red spectral range (Sect. 2.5). In the case of spectroscopic observations, to correct this effect, the frames with the object's spectra are divided by the frames with the accumulated spectra of the built-in lamp (a spectral flat field). In this way, the fringes can be reduced by more than an order of magnitude, which is enough in most cases. We can also get rid of the fringe pattern through division by the flat-field in the case of direct imaging, although using the frames illuminated by the built-in lamp or the twilight sky as a flat field is often not enough, particularly in the case of broad-band filters, since the spectral energy distribution of the night-sky background emission differs markedly from that of the calibration frames. In this case, an optimal imaging technique is to form an image of the averaged interference pattern using a series of all integrations in the corresponding filter during the observing night.

7. Further upgrading of the instrument

A standard autoguiding system using images on the TV-viewing system (Shergin & Maksimova 2001) is used during observations with the 6 m telescope. It allows the displacement of stars in the field to be compensated by the corresponding motions of the entire telescope. This is a slow guiding, since the oscillations of the centers of stellar images at a frequency of 0.1 Hz are suppressed. In 2005, we planned to put into operation a fast guiding system based on a tip-tilt fused quartz plate. This system will allow the oscillations with frequencies up to 10 Hz to be compensated. This will make it possible to significantly reduce the effect of the telescope's natural oscillations, thereby improving the quality of stellar images. For example, using a local tip-tilt corrector at the Nasmyth-2 focus of the 6 m telescope BTA would allow the limiting magnitude of the spectrograph located there to be increased by $0.5 - 1^m$ (Ivanov et al. 2001).

Equipping the spectrograph with a "semi-thin" CCD detector seems promising. This detector combines the advantages of both "thick" (directly illuminated) devices, the absence of an interference pattern, and "thin" devices (back-illuminated) with a high quantum efficiency. Such a detector has a much smaller amplitude of fringes and a higher (up to 80% at 9000Å) sensitivity in the red spectral range, which will allow the SCORPIO efficiency to be increased during near-infrared observations.

8. Conclusions

The high efficiency of the new instrument has been confirmed during its continuous practical use. Over the period from September 2000 through November 2004, observations were performed at SAO on more than 200 nights; the results obtained were used in 26 papers, three Ph.D. and two doctoral dissertations. A more detailed description of the spectrograph and the observing technique can be found in the Internet at *http://www.sao.ru/hq/moisav/scorpio/scorpio.html*. A similar instrument (but without the platform-adapter and the multi-slit unit) produced at the SAO is being successfully used in observations with the 2.6-m Byurakan Astrophysical Observatory telescope (Armenia).

Acknowledgements. We wish to thank the SAO administration for continuous support and attention when the instrument was designed and produced. Dodonov S.N. and Amirkhanyan V.R. for fruitful discussions in making the instrument, Perepelitsyn E.I., Fateev V.I., and Veretenov V.V. who produced and adjusted the individual parts of the spectrograph, the administration of the Institute of Astronomy RAS for making available VPH gratings. This work was supported in part by the "Astronomy" Federal Science and Technology Program (contract no. 40.022.1.1.1101 from February 1, 2002), the INTAS (96-0315) and the Program of the Department of Physical Sciences of the Russian Academy of Sciences. Moiseev A.V. wishes to thank the Russian Science Support Foundation and the Russian Foundation for Basic Research (project no.04-02-16042) for partial support of the work.

References

Afanas'ev V.L., Dodonov S.N., Moiseev A.V., Verkhodanov O.V., Kopylov A.I., Pariiskii Yu.N., Soboleva N.S., Temirova A.V., Zhelenkova O.P., Goss W.M., 2003a, Astronomy Reports, **47**, 377

Afanas'ev V.L., Dodonov S.N., Moiseev A.V., Chavushyan V., Mujica R., Juarez Y., Gorshkov A.G., Konnikova V. K., Mingaliev M. G., 2003b, Astronomy Letters, **29**, 579

Aguerri J. A.L., Debattista V. P., Corsini E.M., 2003, MNRAS, **338**, 465

Amirkhanyan V.R., Afanas'ev V.L., Dodonov S.N., Moiseev A.V., Mikhailov V.P., 2004, Astronomy Letters, **30**, 834

Barden S.C, Arns J.A., Colburn W.S., and Williams J.B., 2000, PASP, **112**, 809

Bessell M.S., 1990, PASP, **102**, 1181

Buzzoni B., Delabre B., Dekker H., et al., 1984, ESO Messenger, (ISSN 0722-6691), Dec. 1984, 9

Courtés G., 1960, Ann. d'Astrophysics, **23**, 115

Courtés G., 1964, AJ, **69**, 325

Fatkhullin T.A., 2002, Bull. Spec. Astrophys. Obs., **53**, 5

Ivanov A.A., Panchuk V.E., Shergin V.S., 2001, Preprint SAO RAS, No.155

Moiseev A.V., 2002, Bull. Spec. Astrophys. Obs., **54**, 74 (astro-ph/0211104)

Nagao T., Kawabata K.S., Murayama T. et al., 2004, AJ, **128**, 109

Neistein E., Maoz D., Rix H.-W., Tonry J.L., 1999, AJ, **117**, p. 2666

Nicklas H., Seifert W., Boehnhardt H., Kiesewetter-Koebinger S., Rupprecht G., 1997, Proc. SPIE, **2871**, in "Optical Telescopes of Today and Tomorrow" (Eds. Arne L. Ardeberg), Nordic Optical Telescope SA (Sweden), 1222

Rozas M., Relano M., Zurita A., Beckman J.E., 2002, A&A, **386**, p. 42

Schmidt G.D., Elston R., Lupie O.L., 1992, AJ, **104**, 1563

Shergin V.S., Maksimova V.M., 2001, Autoguiding Program TV guide. User's guide SAO (`http://www.sao.ru/hq/vsher/vsher_ru.html`)